Open Access

Catalysis Research

LIDSEN Publishing Inc.

Review

Bridging the Gap Between Laboratory Efficiency and Real Wastewater Performance: A Critical Review of Rare-Earth-Doped Metal Oxide Photocatalysts for Dye Degradation

Adeeb Zaid [1], Husam Al-Ziyadi [2], Jacob Wekalao [3], Prasenjit Maity [1, *]

1. School of Engineering & Technology, National Forensic Sciences University (NFSU), Gandhinagar-382007, Gujarat, India; E-Mails: adeeb.phdes2312@nfsu.ac.in; prasenjit.maity@nfsu.ac.in
2. Department of Petroleum Engineering, School of Energy Technology, Pandit Deendayal Energy University, Gandhinagar, Gujarat, India; E-Mail: husamalziyadi@gmail.com
3. Department of Optics and Optical Engineering, University of Science and Technology of China, Hefei, 230026, China; E-Mail: wekalao1998@gmail.com

* **Correspondence:** Prasenjit Maity; E-Mail: prasenjit.maity@nfsu.ac.in

Academic Editor: Aziz Ur Rahim Bacha

Special Issue: Advancements in Photocatalytic Materials for Pollutant Degradation

Catalysis Research
2026, volume 6, issue 3
doi:10.21926/cr.2603011

Received: July 08, 2026
Accepted: September 01, 2026
Published: September 11, 2026

Abstract

Photocatalytic degradation of organic dyes using semiconductor materials has been widely investigated for wastewater treatment. Yet, high activity reported under controlled laboratory conditions does not necessarily translate into practical treatment performance. This review evaluates the hypothesis that rare-earth (RE) doping can improve metal-oxide photocatalysis and examines whether the reported improvements are supported by adequate mechanistic evidence and relevant practical validation. A structured literature search of Web of Science and Scopus identified 29 studies of RE-doped metal oxides for dye degradation. The analysis considered catalyst composition, dopant concentration, morphology, synthesis route, operating conditions, photocatalytic kinetics, mechanistic characterization, mineralization, stability, leaching, and real-wastewater testing. Reported removal efficiencies ranged from 77 to 100%, with a mean of 92.9%; however, these values were not used to rank catalysts

because experimental conditions differed substantially. Mechanistic evidence was classified as direct in 15 studies (51.7%) and partial in 14 (48.3%). PL and XPS were widely reported, whereas EIS and ESR/EPR were used less frequently, indicating that proposed charge-transfer and reactive-species mechanisms are not consistently supported by complementary evidence. TOC analysis was reported in 10 studies (34.5%), none reported apparent quantum yields, and none tested RE-doped photocatalysts with real wastewater. Stability or reuse testing was reported in 20 studies (69.0%), while quantitative rare-earth leaching was reported in only one study (3.4%). These findings show that RE doping can modify photocatalyst properties, but its practical value cannot be established from dye-removal efficiency alone. Standardized reporting, mechanistic validation, real-wastewater testing, long-term stability and leaching assessment, and pilot-scale evaluation are required to advance RE-doped photocatalysts toward reliable wastewater treatment.

Keywords
Photocatalysis; rare-earth doping; metal oxide semiconductors; wastewater treatment; organic dye degradation; charge separation

1. Introduction

Synthetic dyes are widely used in textile, leather, paper, and related industries, and their chemical stability and aromatic structures can make them persistent in aquatic environments [1, 2]. Industrial dye-containing effluents may also contain salts, surfactants, suspended matter, and other dissolved constituents, which further complicate treatment [3]. Conventional approaches, including adsorption, coagulation, membrane separation, and biological treatment, can remove dyes from wastewater but may involve pollutant transfer to another phase or incomplete transformation, thereby requiring additional treatment [4, 5].

Semiconductor photocatalysis has therefore attracted considerable interest as an advanced oxidation approach for the transformation of persistent organic pollutants. Under irradiation, semiconductor materials generate electron-hole pairs that can participate in interfacial redox reactions, producing reactive species capable of attacking organic contaminants [6]. Metal oxides such as TiO_2 and ZnO are among the most widely investigated photocatalysts because of their suitable semiconductor properties and established activity in water treatment [7-11].

Recent studies further demonstrate the development of engineered semiconductor systems for visible-light-driven pollutant degradation, including $ErVO_4$/g-C_3N_4 nanocomposites, magnetic $NiMnFeO_4$/g-C_3N_4 heterostructures, and $NiCrFeO_4$ nanostructures for the removal of dyes and organic pollutants [12-14]. However, their photocatalytic performance is affected by limitations such as restricted visible-light utilization, charge-carrier recombination, and the strong dependence of the reaction on catalyst and operating conditions [15]. Beyond pollutant removal, photocatalytic wastewater treatment is relevant to Sustainable Development Goal 6 (Clean Water and Sanitation), while the development of solar- or visible-light-driven systems may also contribute to SDG 7 (Affordable and Clean Energy) by reducing reliance on externally powered ultraviolet irradiation where suitable solar resources are available [16].

These limitations have motivated several metal-oxide design strategies, including elemental doping, defect engineering, heterojunction formation, nanocomposite construction, and core-shell architecture [17]. For example, doping TiO_2 or ZnO with suitable metal ions can modify electronic states and defect structures, whereas coupling two semiconductors in a heterojunction or nanocomposite can promote interfacial charge separation. Core-shell structures can additionally provide controlled interfaces and facilitate charge-transfer pathways. These approaches can improve light utilization, charge separation, or surface reactivity, but excessive dopant incorporation, unfavorable interfaces, structural complexity, and recombination at defect or interfacial sites can also reduce photocatalytic performance. The effectiveness of each design therefore depends on the relationship between the material structure and the charge-transfer or surface-reaction mechanism rather than on the modification strategy alone [18, 19].

Among these approaches, rare-earth (RE) doping is of particular interest because RE ions can modify the structural, optical, and electronic characteristics of metal oxides through their electronic configurations and interactions with the host lattice. Depending on the dopant and host system, these changes may influence charge-carrier trapping, defect chemistry, light absorption, and surface reactions [20, 21]. Nevertheless, the effect of RE incorporation is not universal and can depend strongly on dopant concentration, host oxide, synthesis route, morphology, and reaction conditions [22, 23].

Several reviews have discussed rare-earth-based photocatalysts, including their synthesis, structural and optical characteristics, and proposed roles in photocatalytic processes [24]. However, these reviews do not provide the same integrated assessment of mechanistic evidence, experimental comparability, mineralization, catalyst stability, rare-earth leaching, and real-wastewater validation as undertaken here. The present review therefore differs by evaluating whether reported improvements associated with RE incorporation are supported by sufficient experimental evidence and whether they remain meaningful when practical treatment requirements are considered.

The present review addresses this need by critically examining rare-earth-doped metal oxide photocatalysts for dye degradation using a defined dataset of 29 studies. The analysis considers material characteristics, synthesis and morphology, operating conditions, photocatalytic kinetics, mechanistic evidence, mineralization, stability, leaching, and real-wastewater validation. Transition-metal doping, metal-oxide nanocomposites, and core-shell structures are considered as comparative modification strategies rather than as additional primary subjects. The review therefore focuses on four questions: how RE incorporation modifies metal-oxide photocatalysts, which proposed mechanisms are experimentally supported, how reported photocatalytic performance should be interpreted under different experimental conditions, and what remains necessary for practical wastewater application. By connecting material modifications with mechanistic evidence and practical performance, this review aims to clarify the actual contributions and limitations of RE doping and to identify priorities for translating laboratory photocatalysis into realistic wastewater treatment.

2. Review Methodology

This review used a structured literature search and critical analysis to evaluate rare-earth-doped metal oxide photocatalysts for organic dye degradation. The analysis focused on material

characteristics, photocatalytic operating conditions, reported performance, mechanistic evidence, and practical applicability.

2.1 Literature Search Strategy

Relevant peer-reviewed studies were identified through searches of Web of Science and Scopus using combinations of terms related to rare-earth elements, metal oxides, photocatalysis, and dye degradation. The search included "rare-earth doped", "lanthanide", and individual rare-earth elements such as Ce, La, Nd, Gd, Sm, Eu, and Yb, combined with "metal oxide", "TiO_2", "ZnO", "SnO_2", "CeO_2", "WO_3", "photocatalytic degradation", and "dye degradation". Backward citation tracking of relevant reviews and primary studies was also performed. The final selected RE-doped studies covered the period 2019-2026.

The literature search was conducted as a structured review rather than as a prospectively registered systematic review. Because the original database exports and record-level screening files were not retained, exact numbers of records identified, duplicates removed, and records excluded at each screening stage could not be reconstructed retrospectively. The final dataset therefore comprises the 29 studies that met the predefined inclusion criteria and contained sufficient experimental information for the comparative analysis.

2.2 Study Selection and Data Extraction

Studies were included when they investigated a defined rare-earth dopant incorporated into a metal oxide photocatalyst, reported quantitative photocatalytic degradation of an organic dye, and provided sufficient experimental information for meaningful comparison. Studies focused only on adsorption or lacking sufficient photocatalytic data were excluded.

A final dataset of 29 RE-doped metal oxide studies was established. Information was extracted on the host oxide, rare-earth dopant and concentration, morphology, synthesis method, structural and optical properties, dye and concentration, catalyst loading, pH, light source, irradiation time, and kinetic data where available. Mineralization indicators (TOC/COD), apparent quantum yield (AQY), stability/reusability, leaching, and real wastewater testing were also recorded when reported. The extracted information is presented in Table 1 and Table S1.

Table 1 Representative rare-earth-doped metal oxide photocatalysts reported for the degradation of organic pollutants, with emphasis on catalyst composition, morphology, operating conditions, photocatalytic performance, mechanistic evidence, and reported limitations.

Host Oxide	RE Dopant	Morphology	Dye	Catalyst Loading (g/L)	Light Source	Time (min)	Removal (%)	Mechanism Evidence	Critical Remarks	Ref
SnO_2	Ce^{3+}	Hollow spheres	MG	1	500 W UV	120	92	Direct (PL + EIS + XPS + Scavenger)	Hollow morphology; $^{\bullet}O_2^-$ main species; 5 cycles	[25]
SnO_2	Ce^{3+}	Nanoparticles	MO	0.1	300 W UV	100	94.5	Partial (PL + XPS + Scavenger)	$^{\bullet}O_2^-$ critical; 4 cycles	[26]
CeO_2	Y^{3+}	Nanocubes	Rose Bengal	1	300 W UV	90	98	Partial (Band gap + XPS + Raman)	V_0 increase; Ce^{3+} 35.3%; no scavenger tests	[27]
ZnO	Ce^{3+}	Nanorods	MB	1.2	350 W Vis	420	96	Partial (PL + XPS)	Ce acts as electron mediator (Ce^{4+}/Ce^{3+}); very long reaction time limits practical applicability; stability 3 cycles	[28]
ZnO	Gd^{3+}	Nanoparticles	Eosin Yellow	1.0	150 W Vis	180	96	Partial (PL + XPS + Scavenger)	Optimal 0.6% Gd; band gap reduced from 3.10 to 2.90 eV; g-C_3N_4 enhances visible light absorption; stability; $^{\bullet}OH$ and $^{\bullet}O_2^-$ radicals involved	[29]

ZnO	Nd^{3+}	Nanoparticles	Acid Yellow-3	0.35	UV	160	91	Partial (PL + XPS)	Hydrothermal synthesis; band gap 3.00 eV; k = 0.0161 min^{-1}; pH 8 optimal; activation energy 33.7 kJ/mol; stability moderate (91% → 72% after 1 cycle)	[30]
TiO_2	La^{3+}	Spherical nanoparticles	MB	0.1	8 W UV	40	88.71	Partial (PL + XPS + Scavenger)	Optimal 1.5% La; crystallite size 19.9 nm; band gap reduced to 2.7 eV; solution-combustion synthesis; stability 5 cycles (77.87%); rate constant 0.048 min^{-1}	[31]
ZnO	Yb^{3+}	Nanodispersion	Tetracycline	0.12	300 W Vis	30	92.6	Direct (PL + XPS + EPR + LC-MS + Scavenger)	Co-precipitation; OVs 38.6%; band gap 3.33 eV; $^{\bullet}O_2^-$ and h^+ dominant; mineralization 47.6%; activity 308.7 mgTC·g^{-1}·h^{-1}; stability 4 cycles (83%)	[32]
ZnO	Gd^{3+}/Nd^{3+}	Nanorods	MB	1.43	300 W Vis	120	93	Partial (PL + XPS + Scavenger)	Co-doping synergy; optimal 1.5%	[33]
TiO_2	La^{3+}	Nanoparticles	MB	0.1	40 W Vis	180 (Vis)	98	Partial (PL + XPS + Scavenger)	Optimal 0.5-2 mol% La; band gap 3.04-2.96 eV; anatase phase; stability 4 cycles (93.5%); La^{3+} on surface as Ti-O-La bonds	[34]

TiO_2	Nd^{3+}	Nanoparticles	MB	0.1	108 W UV	60 (UV)	99.11	Partial (PL + XPS)	Sol-gel ultrasonication; crystallite size 6.41 nm; band gap 3.16 eV; pure TiO_2 has anatase + rutile; Nd-TiO_2 pure anatase; stability 5 cycles (>90%)	[35]
ZnO	Sm^{3+}	Nanocomposites	MB	0.6	48 W UV	150	93.51	Partial (EIS + Scavenger)	Pollutant-specific: Sm enhances MB but not aspirin; EIS shows lowest Rct for 1% Sm (42.91 $\Omega \cdot cm^2$); co-precipitation; hexagonal wurtzite; stability 4 cycles	[36]
TiO_2	Nd^{3+}/Yb^{3+}	Nanoparticles	MB	0.167	Vis	90	93.2	Direct (PL + EIS + XPS + Scavenger)	Hydrothermal; anatase; band gap 3.03 eV; Nd/Yb create oxygen vacancies and redox centres; excellent electrochemical performance (CV, GCD, EIS)	[37]
ZnO	Nd^{3+}	Worm-like nanofibers	MB	1.0	400 W Vis	120	100	Direct (PL + XPS + Scavenger)	Electrospinning-calcination; crystallite size 42.1 nm (optimal); k = 4.780×10^{-2} min^{-1} (MB)/5.291×10^{-2} min^{-1} (CIP); optimal 0.1% Nd; stability 5 cycles	[38]

ZnO	Sm^{3+}	Nanostructures	MB	~2.38	Sunlight	60	77.83	Partial (PL + Scavenger)	Sol-gel; hexagonal wurtzite; 9 wt% also good (65.95%); antibacterial against E. coli, P. aeruginosa, K. pneumoniae, S. aureus; higher Sm increases crystallite size	[39]
WO_3	La^{3+}	Plate-like nanoparticles	MB	1.0	500 W Vis	180	92	Direct (PL + XPS + Scavenger + TOC)	Optimal 3% La; band gap 2.72 eV; rate constant 0.02075 min^{-1} (MB), 0.00739 min^{-1} (TC); $^{\bullet}OH$ dominant; TOC confirms mineralization; stability 4 cycles	[40]
ZnO	La^{3+}	Nanoparticles	Crystal Violet	0.4	12 W Vis	60	92.24	Partial (PL + XPS + Scavenger)	Optimal 2% La; band gap 3.01 eV; rate constant 0.015 min^{-1}; $^{\bullet}OH$ dominant; pH 9 optimal; stability 3 cycles; sol-gel synthesis	[41]
ZnO	Sm^{3+}	Nanoflowers	MB	0.333	Sunlight	90	96	Direct (PL + XPS + Scavenger + TOC)	Co-precipitation; band gap reduced from 3.18 to 3.09 eV; k = 0.2179 min^{-1} (5% Sm); Sm acts as electron trap; TOC removal 87%; stability 5 cycles (90% after 5 cycles)	[42]

$ZnO:TiO_2$	Ce^{3+}	Nanospheres	MB	0.6	Sunlight	90	98	Direct (PL + EIS + ESR + XPS + Scavenger)	Ce doping concentration 1% optimal; band gap reduced from 3.36 to 2.62 eV; excellent photocatalytic performance for both dye and drug degradation	[43]
TiO_2-ZnO	Yb^{3+}/Er^{3+}	Core-shell nanoparticles	MB	0.1	125 W UV	120	98.58	Direct (PL + EIS + ESR + XPS + Scavenger)	Upconversion effect extends light absorption to NIR; band gap narrowed to 2.927 eV; Yb/Er co-doping inhibits anatase-to-rutile phase transition; stability 4 cycles	[44]
ZnO	Er^{3+}	Nanoparticles	MB	0.5	160 W UV	120	99.77	Direct (PL + XPS + Scavenger)	Green synthesis using Mangifera indica gum; Er^{3+} creates oxygen vacancies; hydroxyl radicals ($^{\bullet}OH$) are the main active species; stability 3 cycles; high reusability for MB	[45]
ZnO	Er^{3+}	Hexagonal prism-like nanoparticles	MB	0.3	32 W UV	60	87.9	Direct (PL + EIS + XPS + Scavenger)	Optimal doping 3 wt%; $O_2^{\bullet-}$ is dominant reactive species; GC-MS confirms degradation pathway; excellent stability (93% after 4 cycles); antibacterial activity against both Gram-positive and Gram-negative bacteria	[46]

TiO_2	Eu^{3+}	Hierarchical nanoparticles	Congo Red	0.4	100 W (UV)	75	97	Partial (PL + XPS + Scavenger)	Anatase phase; crystallite size 5.18-5.05 nm; band gap 3.40-3.43 eV; pH 3 optimal; stability 4 cycles	[47]
TiO_2	Eu^{3+}	Thin films (on p-Si)	Amido Black 10B	Thin film	UV	120	98.94	Direct (PL + EIS + XPS + Scavenger)	Optimal 0.1 wt% Eu; k = 0.036 min^{-1}; pH 3.5 optimal; EIS confirms lower charge transfer resistance; HPLC confirms mineralization	[48]
TiO_2	Gd^{3+}	Nanoparticles	Quinoline	0.5	300 W UV	180	84	Direct (PL + EIS + XPS + Scavenger)	Optimal 1.5% Gd; SA 174 m^2/g (55% increase); band gap 3.06 eV; $^{\bullet}OH$ dominant species; stability 4 cycles (80.3%)	[49]
ZnO	Gd^{3+}	Nanoparticles	MB	0.5	500 W UV	120	89	Partial (EIS)	Optimal 7.5% Gd; k = 0.00723 min^{-1}; band gap 3.07 eV; EIS shows reduced charge transfer resistance; stability 5 cycles	[50]
ZrO_2	Nd^{3+}	Nanoparticles	RhB	2.0	300 W Vis	120	77	Direct (PL + EIS + XPS + Scavenger)	Co-precipitation; band gap 1.23 eV; k = 0.0144 min^{-1} (MB)/0.00944 min^{-1} (RhB)/0.0021 min^{-1} (AC); holes (h^+) dominant species; stability 3 cycles	[51]

TiO_2	Sm^{3+}	Nanoparticles	RhB	0.4	Sunlight	120	89	Direct (PL + EIS + XPS + Scavenger)	Photolysis synthesis; crystallite size 4.56 nm; band gap 2.86 eV; k = 0.02094 min^{-1}; pH 12 optimal; HPLC/LC-MS confirms N-deethylation pathway; stability 5 cycles	[52]
TiO_2	Ho^{3+}/Yb^{3+}	Nanoparticles	RhB	0.1	300 W UV	130	91	Direct (PL + XPS + Scavenger)	Hydrothermal; anatase phase; PL intensity decreases with co-doping; band gap 3.15 eV; suppressed e^{-}-h^{+} recombination	[53]

2.3 Comparative and Mechanistic Analysis

The extracted data were interpreted in light of differences in experimental conditions, including catalyst loading, dye concentration, pH, irradiation conditions, reaction time, and kinetic parameters. Because irradiation intensity at the reaction surface was not consistently reported, direct normalization of light input was not possible. Reported removal efficiencies were therefore not used alone to rank photocatalysts.

Mechanistic interpretations were evaluated according to the experimental evidence reported in each study. Mechanisms supported by complementary characterization or experimental measurements were distinguished from interpretations inferred mainly from photocatalytic performance. This assessment considered evidence such as photoluminescence, electrochemical measurements, XPS, ESR/EPR, scavenger tests, and photocurrent measurements. The detailed classification and its results are presented in Section 6.1.

For other reported variables, catalyst loading, pollutant concentration, and solution volume were retained as explicit comparison parameters in the extracted dataset; however, a single normalized activity metric was not calculated because the studies differed substantially in reactor configuration, irradiation conditions, and reporting completeness.

Representative studies on transition-metal doping, nanocomposites, and core-shell structures were considered separately to provide comparative context for rare-earth doping rather than as additional exhaustive datasets.

2.4 Quality Assessment and Limitations

Study quality was assessed based on the completeness of experimental reporting and the availability of relevant control experiments, replication or uncertainty information, and supporting mechanistic evidence. To reduce selection bias, predefined search terms and inclusion/exclusion criteria were consistently applied across searches of Web of Science and Scopus, and backward citation tracking was used to identify relevant studies that the database searches may not have retrieved. Publication bias was not statistically assessed because the review was not designed as a quantitative meta-analysis; therefore, preferential publication of positive photocatalytic results cannot be excluded. These limitations were considered when interpreting the reported performance and mechanistic evidence.

A formal quantitative meta-analysis was not performed due to substantial heterogeneity across studies in catalyst composition, dye characteristics, catalyst loading, irradiation conditions, reactor configuration, reaction time, and reported response parameters. These differences prevent reliable pooling of effect sizes without introducing substantial assumptions or potentially misleading comparisons. A bibliometric analysis was also outside the scope of this review, which focuses on scientific evidence, mechanistic understanding, photocatalytic performance, and practical applicability rather than publication trends or research-network mapping.

3. Why Dyes Persist and Conventional Treatments Fall Short

Synthetic dyes are widely used in textile, leather, paper, and other manufacturing processes, and their chemical stability and aromatic structures can make them persistent in aquatic environments

[4]. During industrial processing, a fraction of the applied dye may remain in wastewater, resulting in strongly coloured effluents that can contain mixtures of dyes and other dissolved constituents. Their removal is therefore complicated not only by the chemical stability of individual dye molecules but also by the variable composition of industrial effluents.

Conventional treatment processes can provide effective separation or transformation of pollutants, but each approach has practical limitations. Adsorption and membrane processes can remove dyes from the aqueous phase, but they generate spent adsorbents or concentrated retentate that require subsequent management [54]. Chemical oxidation can rapidly transform dye molecules, although the extent of transformation depends on the oxidant and operating conditions, and incomplete oxidation may leave intermediate products. Biological treatment can be cost-effective for suitable wastewater matrices, but its performance may decrease under high salinity, variable pH, and the presence of inhibitory or poorly biodegradable compounds [55, 56].

These limitations have motivated interest in advanced oxidation processes such as semiconductor photocatalysis, which can generate reactive species under irradiation and promote the transformation of organic pollutants. However, photocatalysis should not be considered a universal replacement for conventional treatment. Its effectiveness depends on catalyst properties, irradiation conditions, pollutant concentration, water chemistry, and reactor operation. This distinction is central to the present review: high dye removal under controlled model-solution conditions does not necessarily demonstrate mineralization, performance in real wastewater, or industrial feasibility. The following sections therefore first establish the fundamental factors governing photocatalytic activity and then examine how metal-oxide modification, particularly rare-earth doping, affects these factors.

4. Fundamentals of Photocatalysis

Semiconductor photocatalysis is based on the generation and subsequent utilization of photogenerated charge carriers. When incident photons provide energy equal to or greater than the semiconductor band gap, electrons are promoted from the valence band (VB) to the conduction band (CB), leaving holes in the VB. The generated electrons and holes can migrate toward the catalyst surface and participate in oxidation-reduction reactions, provided that they avoid bulk or surface recombination. Thus, photocatalytic performance depends not only on light absorption but also on charge separation, transport, surface reactions, and the surrounding reaction environment [57-59]. The formation of charge carriers does not necessarily result in efficient pollutant degradation because a substantial fraction may recombine before reaching reactive surface sites. Consequently, the useful photocatalytic process involves a sequence of coupled steps: photon absorption, charge generation and separation, carrier migration, interfacial redox reactions, formation of reactive species, and transformation of the pollutant. Figure 1 summarizes these processes for metal-oxide photocatalysts [60, 61].

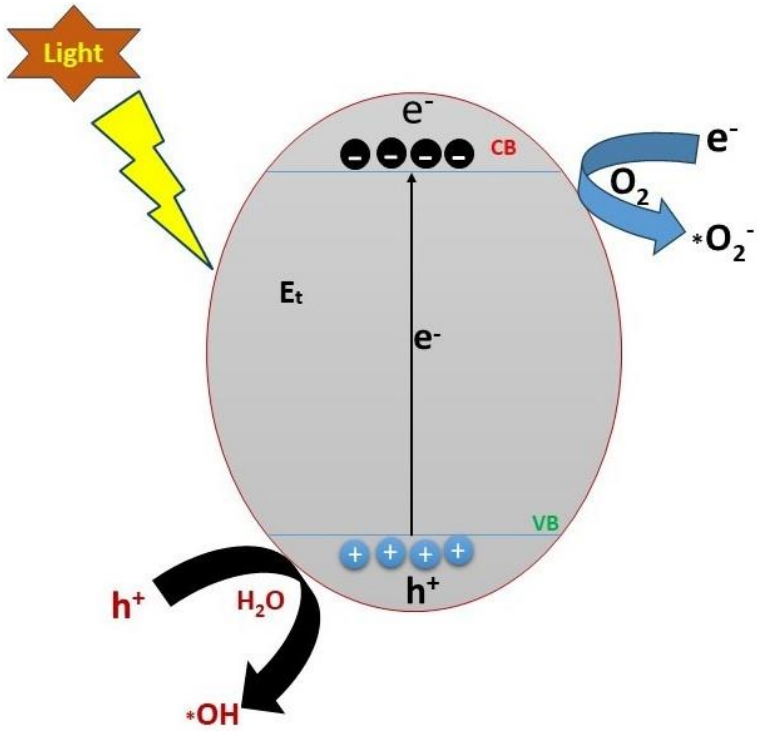

Figure 1 Mechanism of photocatalytic degradation using semiconducting metal oxides [62].

4.1 Band Structure and Light Absorption

Band-gap energy and band-edge positions determine which wavelengths can excite a semiconductor and whether the resulting charge carriers possess sufficient redox potential for surface reactions. TiO_2, ZnO, and SnO_2 have relatively wide band gaps and therefore absorb predominantly in the ultraviolet region [57, 58]. Narrowing the band gap can extend light absorption into the visible region, but this modification may also alter the redox potential and structural stability of the material.

This trade-off is important when evaluating photocatalyst modification. Increasing visible-light absorption does not necessarily produce higher photocatalytic activity if the resulting band positions no longer provide sufficient driving force for the required oxidation or reduction reactions. Therefore, effective band-structure engineering should balance light harvesting, redox potential, and structural stability rather than target band-gap narrowing alone. Figure 2 compares representative semiconductor band gaps and illustrates the relationship between optical absorption and photocatalytic activation.

Figure 2 Different band gaps of semiconducting metal oxides [17].

4.2 Charge Carrier Separation and Transport

Following photoexcitation, electrons and holes must reach reactive surface sites before recombination. Their transport is influenced by crystallinity, particle size, morphology, defect states, and surface structure. Defects can either promote or hinder charge separation depending on their concentration and electronic character. For example, oxygen-vacancy engineering has been reported to create trapping states that can influence carrier separation, whereas excessive defect formation may introduce recombination centres [63]. This dual behaviour is important for the modification strategies discussed later in this review. A change in photoluminescence intensity or defect concentration should not, by itself, be interpreted as proof of improved charge separation. Stronger mechanistic conclusions require complementary evidence from techniques such as photoluminescence, electrochemical measurements, transient spectroscopy, or radical-scavenging experiments. This distinction is particularly relevant when evaluating the proposed mechanisms of rare-earth doping.

4.3 Generation and Role of Reactive Oxygen Species (ROS)

Once charge carriers reach the catalyst surface, they can participate in reactions with adsorbed water, hydroxyl groups, dissolved oxygen, and pollutants. Conduction-band electrons can reduce dissolved oxygen to superoxide-related species. At the same time, valence-band holes can oxidize water or surface hydroxyl groups to generate hydroxyl radicals when the corresponding redox potentials are sufficiently favorable. These reactive species can then participate in oxidation reactions leading to dye transformation [64]. The relative contribution of individual reactive species is not universal. It depends on band-edge positions, pH, dissolved oxygen, surface chemistry, adsorption behaviour, and the specific catalyst-pollutant system. Therefore, assignment of $^{\bullet}OH$, $^{\bullet}O_2^-$, holes, or other reactive species should be based on appropriate experimental evidence, such as scavenger experiments, ESR/EPR measurements, or complementary spectroscopic analysis, rather than inferred from removal efficiency alone. This evidence-based distinction is applied throughout the subsequent analysis of RE-doped photocatalysts.

4.4 Photocatalytic Degradation Mechanisms of Synthetic Dyes

Photocatalytic dye degradation generally involves a sequence of molecular transformations rather than a single reaction step. Initial reactions may disrupt chromophoric groups, followed by transformation of aromatic fragments and, under sufficiently strong oxidation conditions, further conversion toward smaller molecules and mineralization products. The pathway depends on the dye structure, substituent groups, catalyst surface, reactive species, and reaction conditions.

The reaction pathway can also differ among dye classes. For example, azo dyes can undergo cleavage of the azo bond under appropriate photocatalytic conditions [65]. However, the disappearance of the parent dye or loss of colour does not by itself demonstrate complete mineralization. Detection of intermediates, TOC/COD reduction, or other product analyses is required to establish the extent of mineralization and to evaluate whether potentially persistent or toxic transformation products remain [66].

4.5 Factors Affecting Photocatalytic Efficiency

Photocatalytic performance results from the interaction between catalyst characteristics, including surface area, crystallinity, morphology, defect structure, and surface chemistry, and operating conditions such as pH, pollutant concentration, catalyst loading, irradiation wavelength and intensity, reaction time, and temperature [67, 68]. These parameters can influence light absorption, adsorption, charge-carrier behaviour, and reactive-species formation, and their effects are often interdependent.

For example, pH can modify catalyst surface charge and pollutant speciation, while increasing pollutant concentration can reduce photon penetration and alter the availability of reactive surface sites. Catalyst loading also requires optimization, as insufficient catalyst loading limits the available active surface, whereas excessive loading can increase light scattering and attenuation [69-71]. In complex wastewater, dissolved organic matter and other constituents can additionally consume reactive species or interfere with light penetration, altering photocatalytic performance differently from that observed in simplified dye solutions [72, 73].

These dependencies have important implications for cross-study comparison. A reported removal percentage cannot be interpreted independently of catalyst loading, pollutant concentration, pH, irradiation conditions, reaction time, and wastewater composition. Accordingly, the comparative analysis in this review considers these conditions where they were reported rather than ranking photocatalysts solely by removal efficiency.

5. Metal Oxide Nanoparticles (MONPs) as Photocatalysts

Metal oxide nanoparticles, particularly TiO_2 and ZnO, are widely investigated for photocatalytic wastewater treatment because their semiconductor properties support light-induced charge generation and surface redox reactions [74-77]. Their photocatalytic behaviour is strongly influenced by crystallinity, morphology, surface properties, defect structure, and band alignment rather than by chemical composition alone. These materials therefore provide useful reference systems for evaluating the effects of subsequent modification strategies.

5.1 Structural and Optical Properties Influencing Activity

The photocatalytic behaviour of metal oxide nanoparticles depends on crystallinity, particle size, morphology, surface hydroxylation, defect concentration, and electronic structure. Morphological characteristics can influence light scattering, active-site accessibility, and charge-transport pathways [78]. A recent study of morphology-engineered ZnO tetrapods further illustrates this structure-performance relationship, showing that a highly crystalline three-dimensional architecture with controlled defect characteristics can provide rapid photocatalytic degradation even without compositional doping [79]. Surface hydroxyl groups can participate in the formation of reactive species, while defects may act as charge-trapping sites; however, their effects depend on defect type and concentration [80, 81].

CeO_2 provides an illustrative example of this balance. Oxygen defects and associated Ce^{3+} species can modify the optical and electronic properties of CeO_2, whereas excessive defect formation may promote recombination rather than improve photocatalytic activity [82-85]. Thus, defect engineering should be controlled rather than treated as inherently beneficial.

TiO_2 also illustrates the importance of crystal structure. It occurs in anatase, rutile, and brookite polymorphs, and differences in crystal structure can influence charge-carrier behaviour and surface reactivity. ZnO has also attracted extensive attention due to its favourable photocatalytic properties, although its stability under irradiation remains an important consideration [76, 77].

These examples show that the performance of pristine metal oxides cannot be attributed to a single material parameter. Morphology, crystal structure, defect chemistry, surface properties, and operating conditions can interact, making it difficult to directly attribute performance changes to a single structural feature.

5.2 Practical Limitations of Pristine Metal Oxides

Despite their useful photocatalytic properties, pristine metal oxides have limitations that restrict their practical application. TiO_2, ZnO, and SnO_2 have relatively wide band gaps and therefore absorb predominantly in the ultraviolet region, limiting their direct use of visible solar radiation [57, 83-85]. Extending light absorption toward the visible region can improve photon utilization, but changes in the band structure may also affect the redox driving force and material stability. ZnO presents an additional stability concern because photocorrosion can occur during irradiation, potentially resulting in catalyst dissolution and loss of material from the treatment system [86]. More generally, catalyst performance can decrease when the reaction environment differs substantially from the simplified conditions used in laboratory experiments. For example, TiO_2- and ZnO-based photocatalytic treatment of textile effluents has shown that wastewater composition can influence treatment performance [87].

These limitations indicate that high activity of a pristine oxide is not sufficient to establish practical suitability. Catalyst stability, light utilization, interaction with the pollutant, and behaviour in complex wastewater must also be considered. These limitations illustrate why modification strategies are being investigated to improve the functional properties and practical performance of metal oxide photocatalysts, as summarized schematically in Figure 3.

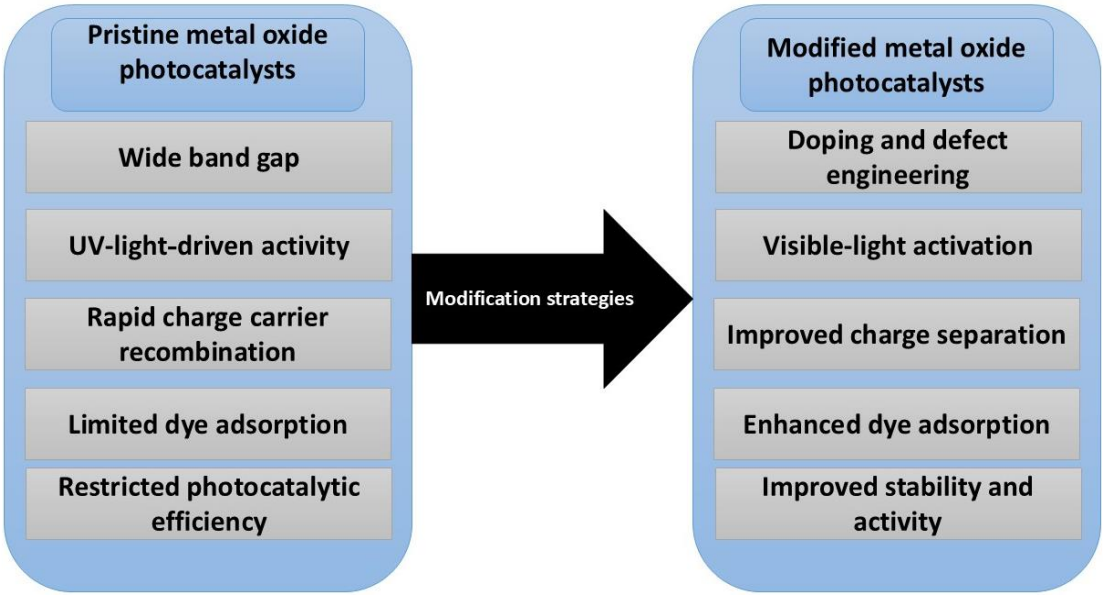

Figure 3 Comparison of pristine and modified metal oxide photocatalysts [86].

5.3 Motivation for Performance Improvement Strategies

The limitations of pristine metal oxides have motivated modification strategies including elemental doping, defect engineering, heterojunction formation, nanocomposite construction, and morphology control. These approaches aim to modify specific properties such as light absorption, charge-carrier separation, surface reactivity, or structural stability.

However, modification does not guarantee improved photocatalytic performance. Changes in defect density, morphology, surface chemistry, or band structure can produce beneficial or adverse effects depending on the material and operating conditions [86, 88]. Therefore, modification strategies should be evaluated mechanistically rather than solely by changes in reported dye-removal percentages.

Among these approaches, rare-earth doping is particularly relevant because RE ions can alter the electronic and structural characteristics of metal oxides through their distinctive electronic configurations and interactions with the host lattice. The following section therefore examines RE-doped metal oxides while considering the host oxide, dopant concentration, morphology, synthesis route, operating conditions, and available mechanistic evidence.

6. Rare-Earth-Doped Metal Oxide Nanoparticles

Rare-earth (RE) doping has been widely investigated to modify the structural, optical, and electronic properties of metal oxide photocatalysts. The partially filled 4f orbitals of RE ions can introduce localized electronic states and influence charge-carrier transfer, defect formation, light absorption, and surface reactions. However, the effect of RE incorporation is not uniform across host oxides and can vary with the dopant, its concentration, host structure, synthesis route, morphology, and reaction conditions [24, 89-91].

To address this variability, Table 1 presents representative RE-doped metal oxide photocatalysts and focuses on parameters relevant to cross-study interpretation, including host oxide, RE dopant, morphology, catalyst loading, irradiation conditions, removal efficiency, mechanistic evidence, and critical observations. The corresponding experimental details are provided in Table S1, including pollutant concentration, solution volume, pH, band-gap energy, surface area, kinetic constants, PL, EIS, ESR, XPS, scavenger tests, TOC, AQY, real-wastewater testing, stability, leaching, and the assigned level of mechanistic confidence.

The 29 studies summarized in Table 1 report substantial photocatalytic activity for RE-doped TiO_2, ZnO, SnO_2, WO_3, ZrO_2, and CeO_2 systems under their respective experimental conditions. Reported removal efficiencies ranged from 77 to 100%, with a mean of 92.9% and a median of 93.2%. These values, however, cannot be treated as direct measures of intrinsic catalyst superiority because catalyst loading, pollutant concentration, irradiation source, reaction time, and other operating variables differ among studies. The analysis therefore focuses on patterns in mechanistic evidence, structural and morphological effects, dopant concentration, and practical validation rather than ranking catalysts solely by removal efficiency. Accordingly, reported removal efficiencies are interpreted in conjunction with catalyst loading, pollutant concentration, solution volume, irradiation conditions, and reaction time wherever these parameters were available, rather than being treated as directly comparable intrinsic activities.

6.1 Mechanistic Influence of Rare-Earth Incorporation

RE incorporation can influence photocatalytic behaviour by altering charge-carrier trapping, defect chemistry, interfacial charge transfer, and surface reactions. The studies compiled in Table 1, however, do not provide the same level of evidence for these effects. Among the 29 studies, 15 (51.7%) were classified as providing direct mechanistic evidence, whereas 14 (48.3%) provided partial evidence. This distinction is important because improved dye removal alone does not establish the pathway responsible for the observed enhancement.

The type of characterization used to support the proposed mechanisms also varies considerably across the dataset. Among the 29 studies, PL analysis was reported in 27 studies (93.1%), XPS in 27 studies (93.1%), EIS in 11 studies (37.9%), ESR/EPR in 3 studies (10.3%), and scavenger tests in 22 studies (75.9%) (Table 1; Table S1). The frequent use of PL and XPS indicates that changes in optical and surface properties are commonly examined. However, these techniques alone do not establish a complete charge-transfer pathway or identify the reactive species responsible for degradation. More convincing mechanistic assignments are obtained when complementary evidence, such as electrochemical measurements, radical-trapping experiments, and spectroscopic identification, is combined.

The individual studies also show that the effect of RE incorporation is system-dependent. For example, Ce-doped SnO_2 hollow spheres were supported by PL, EIS, XPS, and scavenger evidence. In contrast, the Ce-doped SnO_2 nanoparticles in another study relied on a more limited combination of PL, XPS, and scavenger tests [25, 26]. Similarly, the Gd/Nd co-doped ZnO system provided only partial mechanistic evidence despite the reported photocatalytic improvement [27]. These differences illustrate why the presence of an RE dopant cannot, by itself, be taken as evidence of a particular charge-transfer or radical-generation pathway.

The quantitative comparison further supports this caution. The mean removal efficiency was 92.7% for studies classified as providing direct mechanistic evidence and 93.1% for those classified as providing partial mechanistic evidence. Thus, the two groups showed very similar reported removal efficiencies despite a clear difference in the amount of mechanistic support. High photocatalytic removal therefore does not necessarily indicate stronger mechanistic verification. The result also underscores the need to distinguish between measured evidence and mechanistic interpretation when comparing RE-doped photocatalysts. Because most studies reported lamp power rather than irradiance at the reaction surface, direct normalization of the incident light intensity across studies was not possible; therefore, reported removal efficiencies are interpreted within their respective experimental conditions rather than as directly comparable intrinsic activities. The distribution of mechanistic evidence and practical validation across the reviewed studies is summarized in Figure 4, highlighting the extent to which key performance and validation parameters were reported.

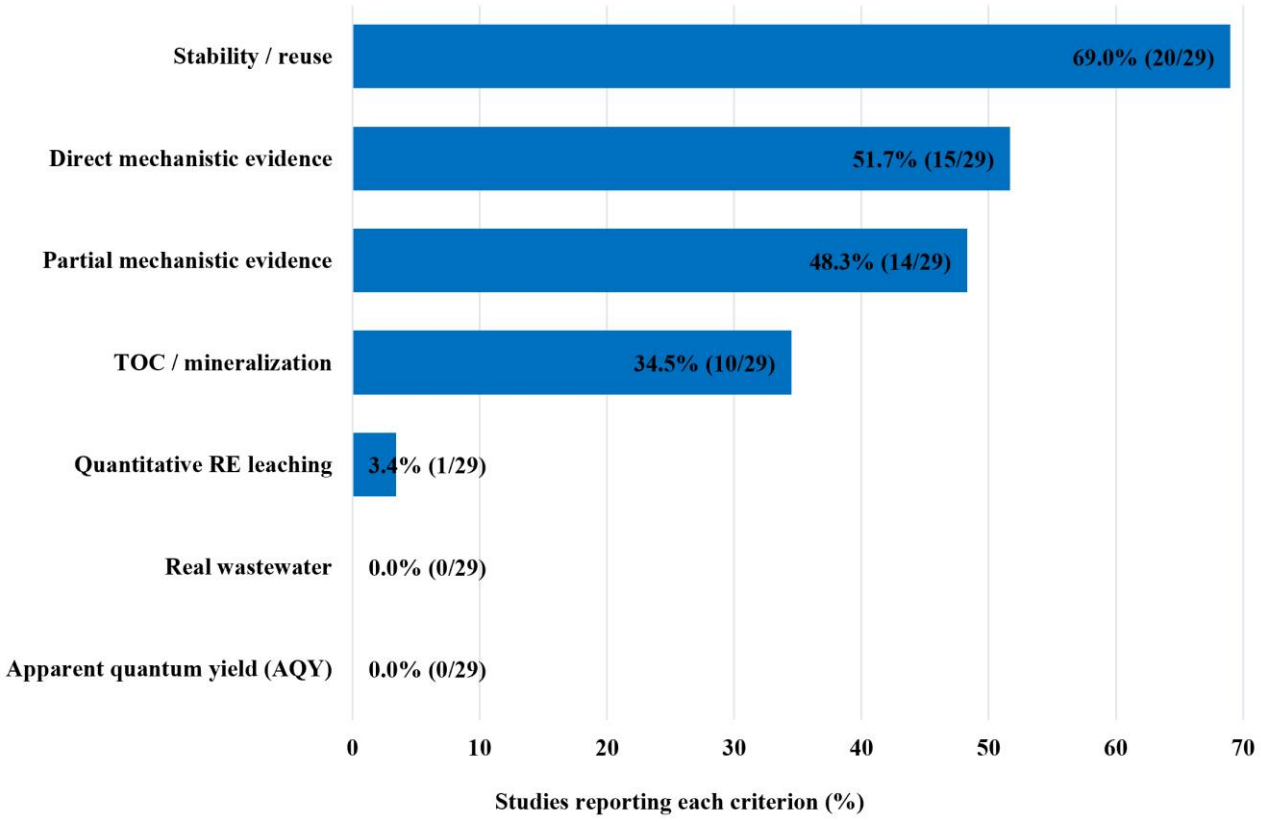

Figure 4 Evidence strength and practical validation reported across the 29 rare-earth-doped metal oxide photocatalyst studies reviewed.

A further limitation is the relatively low use of techniques that can provide complementary evidence for charge-transfer behaviour and reactive oxygen species. Only 11 of the 29 studies included EIS, 3 included ESR/EPR, and none reported an apparent quantum yield (AQY). TOC analysis was reported in 10 studies (34.5%), indicating that mineralization was assessed in substantially fewer studies than dye removal. The nearly equal distribution between direct and partial mechanistic evidence therefore suggests that mechanistic claims remain unevenly supported across the reviewed RE-doped systems.

In this review, reported dye removal is treated as decolourisation or pollutant removal unless supported by TOC, COD, or other product-analysis data; therefore, removal efficiency alone is not interpreted as evidence of complete mineralization or toxicity reduction.

6.2 Structural, Optical, and Morphological Effects of Rare-Earth Incorporation

RE incorporation can modify photocatalytic behaviour by altering crystal structure, particle morphology, surface properties, and optical response. The current dataset shows substantial morphological diversity, including hollow spheres, nanorods, nanocubes, nanospheres, core-shell structures, nanoflowers, nanofibers, thin films, and nanodispersions (Table 1). This variation is important because morphology is not an independent parameter in most studies; it is closely linked to the synthesis route, dopant concentration, and host oxide.

The Ce-doped SnO_2 studies illustrate the structural diversity reported across the literature. One study prepared Ce-doped SnO_2 as hollow spheres with a measured surface area of 62.62 $m^2\ g^{-1}$,

whereas another prepared Ce-doped SnO_2 as nanoparticles [25, 26]. The hollow-sphere study also showed that Ce incorporation did not alter the overall hollow morphology, indicating that the observed structure cannot be attributed to doping alone [25]. These results highlight the need to consider synthesis route and pre-existing particle architecture when interpreting the role of RE incorporation. The available studies do not allow the individual contributions of morphology, dopant concentration, and reaction conditions to be separated.

Similar morphological diversity occurs for ZnO. Gd/Nd co-doped ZnO was prepared as nanorods, Ce-doped ZnO as nanorods and nanospheres, and Er-, La-, Nd-, and Sm-containing ZnO systems were reported as nanoparticles, nanoflowers, nanofibers, nanocomposites, or other nanostructures [28-32]. These studies indicate that RE incorporation can result in different final morphologies rather than a single characteristic structural form. The variation also suggests that the synthesis method remains an important factor in interpreting the role of the dopant.

Changes in optical properties are also frequently reported. Band-gap values were available for 26 of the 29 studies (89.7%), indicating that optical characterization is much more commonly reported than surface-area measurements. Several systems show lower band-gap values after RE modification or report optical features associated with improved visible-light response. For example, the Ce-doped ZnO/TiO_2 system reported a band gap of 2.62 eV, while the Yb/Er co-doped TiO_2-ZnO system showed a band gap of 2.92 eV [92, 93]. Gd-doped ZnO systems also showed band-gap values around 2.9-3.1 eV depending on the catalyst composition and preparation conditions [33, 94, 95]. These results support the view that RE incorporation can alter the optical response, but they do not establish that band-gap reduction alone is responsible for the observed photocatalytic activity.

The relationship between optical properties and photocatalytic performance is further complicated by the different irradiation conditions used in the studies. The dataset includes UV, visible-light, sunlight, and mixed irradiation conditions. Consequently, a lower reported band gap cannot be interpreted independently of the incident light spectrum, irradiation power, exposure time, and catalyst loading. This is particularly important for studies reporting visible-light or solar-light activity, where enhanced absorption may contribute to performance but does not by itself demonstrate more efficient charge separation or reactive-species formation.

Surface-area data provide another example of the limitations in the current literature. Only 6 of the 29 studies reported specific surface area values in the extracted dataset. The available values vary widely, but the limited number of observations and differences in morphology, catalyst loading, pollutant concentration, and irradiation conditions prevent the establishment of a meaningful quantitative relationship between surface area and dye removal. The structural information should therefore be interpreted as supporting evidence rather than as a basis for ranking the catalysts.

Taken together, the dataset indicates that RE incorporation can affect morphology and optical properties, but these changes are strongly coupled with host composition and synthesis conditions. The evidence does not support a single structural or optical feature as the dominant explanation for improved photocatalytic performance. Instead, the reported activity appears to reflect the combined effects of composition, morphology, optical response, surface properties, and charge-carrier behaviour, with their relative contributions varying among RE-oxide systems.

Crystallographic evidence also shows that the effect of RE incorporation is host-dependent. For example, the TiO_2 systems reported in the dataset include anatase phases, while ZnO systems retain the hexagonal wurtzite structure [34-37]. In one Nd-doped TiO_2 system, the undoped material contained anatase and rutile phases, whereas the Nd-doped material was reported as pure anatase.

Other studies reported changes in crystallite size following RE incorporation, including the Nd-doped ZnO and Sm-doped ZnO systems [38, 39]. These observations indicate that structural changes accompanying RE incorporation should be evaluated experimentally rather than inferred solely from photocatalytic performance.

Pore-size information was not reported in the reviewed studies and therefore could not be included in the comparative analysis.

The synthesis route also influences the structural characteristics of RE-doped metal oxides. The reviewed studies employed sol-gel, hydrothermal, precipitation, combustion, electrospinning-based, and solvothermal approaches; a detailed comparison of their principal advantages, limitations, and typical structural effects is provided in Table S2. Sol-gel and precipitation routes provide relatively simple preparation and compositional control, whereas hydrothermal processing can promote controlled crystal growth and morphology. Combustion routes offer rapid synthesis but may provide less control over particle growth, while electrospinning-based methods are useful for producing one-dimensional structures. However, these effects cannot be attributed solely to the synthesis route because the resulting morphology and photocatalytic performance are also affected by the host oxide, RE concentration, calcination conditions, and reaction parameters. Thus, the present dataset supports the synthesis route as an important structural variable but does not justify ranking one method as universelectronic structureally superior.

6.3 Optimum Dopant Concentration and Performance Window

The photocatalytic response of RE-doped metal oxides varies with dopant concentration, but the present dataset does not support a single optimum concentration applicable across different host oxides. The reported RE concentrations span approximately 0.1-10%, with several studies identifying an optimum within this range for their specific catalyst system (Table 1; Table S1). For example, the La-doped TiO_2 systems reported optimum concentrations of 1.5-2%, while Gd/Nd co-doped ZnO showed an optimum of 1.5% [31, 34, 35, 40, 41]. Nd-doped ZnO and Sm-doped ZnO systems also showed concentration-dependent activity, but their reported optimum values differed between studies and morphologies [38, 39, 42].

This variation is also evident when the same RE element is introduced into different host oxides. The optimal concentration of La^{3+}, Nd^{3+}, and Sm^{3+} is not constant across TiO_2, ZnO, WO_3, and ZrO_2 systems (Table 1). Such differences indicate that the effect of dopant concentration depends on the host lattice, synthesis route, morphology, and reaction conditions. Therefore, the concentration associated with the highest removal in one system cannot be directly transferred to another.

At low concentrations, RE incorporation may modify the electronic structure and provide sites that influence charge-carrier behaviour. Increasing the dopant concentration can produce a different response if excessive incorporation alters crystallinity, promotes defect accumulation, or changes the surface structure. The available studies, however, do not provide sufficient standardized data to establish a quantitative relationship between concentration and performance across the full dataset. This limitation is particularly important because the studies use different host materials, pollutants, irradiation conditions, and catalyst loadings.

The dataset also shows that high photocatalytic activity is not restricted to a narrow range of dopant concentration. Several catalysts achieved removal efficiencies above 95% at concentrations below 2%, whereas other systems showed high activity at higher concentrations. For example, Ce-

doped SnO_2, La-doped TiO_2, Nd-doped TiO_2, and Sm-doped ZnO achieved high reported removal under their respective experimental conditions at different dopant levels [34, 35, 42]. These results further argue against defining a universal concentration window solely from reported removal percentages.

A further limitation is that concentration optimization is not consistently investigated over a sufficiently broad range. Some studies compare several dopant concentrations, whereas others report only one selected composition. Consequently, the concentration identified as "optimal" in an individual study should be interpreted as an experimental optimum for that specific catalyst and reaction system rather than as a general optimum for RE doping. Systematic concentration series, combined with structural, spectroscopic, and kinetic measurements, would provide a stronger basis for identifying the concentration range at which RE incorporation improves charge separation without introducing adverse recombination or structural effects.

Real-wastewater validation remains largely unexplored in the reviewed RE-doped systems. None of the 29 studies included in the present dataset reported photocatalytic testing using real wastewater. The reported efficiencies therefore reflect performance in controlled model solutions and cannot be assumed to represent behaviour in complex effluents. In real textile wastewater, dissolved organic matter, inorganic ions, salinity, turbidity, and surfactants may compete for active sites, attenuate light penetration, or consume reactive species, potentially reducing photocatalytic performance. This lack of real-effluent validation limits assessment of the practical applicability of RE-doped metal oxide photocatalysts.

Catalyst stability and rare-earth leaching were also insufficiently evaluated across the dataset. Stability or reuse testing was reported for 20 of the 29 studies (69.0%), whereas quantitative leaching measurements were reported in only one study (3.4%). Thus, although repeated-use performance was examined in a substantial proportion of the literature, evidence for rare-earth release during photocatalytic operation remains very limited. More systematic evaluation of activity retention, structural stability, and rare-earth leaching during repeated cycles is needed to assess the long-term reliability of RE-doped metal oxide photocatalysts.

Environmental safety remains insufficiently assessed for RE-doped metal oxide photocatalysts. The reviewed studies did not report systematic ecotoxicity assessments of the photocatalysts or released rare-earth species, and nanoparticle release was not adequately evaluated. Therefore, high photocatalytic removal efficiency should not be interpreted as evidence of environmental safety. Future studies should combine photocatalytic performance with measurements of rare-earth release, nanoparticle stability, and relevant ecotoxicity endpoints, particularly during repeated use.

7. Transition-Metal Doping in Metal Oxide Nanoparticles

Transition-metal (TM) doping is considered here as a comparative modification strategy for examining how dopant electronic structure and defect chemistry can influence metal-oxide photocatalysis relative to rare-earth incorporation. TM dopants can modify the electronic and defect structure of oxide semiconductors, with the resulting photocatalytic response depending on the dopant identity, concentration, host lattice, and incorporation environment [96]. These effects are relevant to the present review because they provide a useful contrast with the electronic and structural modifications produced by rare-earth ions.

First-principles calculations on TM-doped TiO_2 have shown that transition-metal incorporation can alter the electronic structure and the calculated band gap of the host, demonstrating that the effect of doping depends on the identity of the dopant and its interaction with the host lattice [97].

The structural and electronic effects of TM incorporation may also involve defect states, including oxygen-vacancy-related states. Still, their influence on photocatalysis is not unidirectional: defect states can contribute to sub-band-gap absorption or carrier trapping, while excessive or deep defect states may instead promote non-radiative recombination [98]. Therefore, Section 7 does not assume that TM incorporation or defect formation necessarily enhances photocatalytic activity; the relevant mechanism must be established from the experimental or computational evidence reported for each system.

7.1 Representative Evidence and Comparison with Rare-Earth Doping

Representative transition-metal (TM)-doped metal oxides show that the photocatalytic effect of TM incorporation is strongly dependent on the dopant and host system. For example, Cu- and Ni-doped ZnO showed different methyl orange degradation efficiencies and kinetic constants under the same experimental framework, with Ni/ZnO providing the highest reported activity among the tested compositions [99]. Ni-doped ZrO_2 has also been investigated as a concentration-dependent photocatalyst for organic pollutant removal, while Ni-doped WO_3 nanoplates provide another example of TM modification of a metal oxide host [100, 101].

These studies indicate that TM incorporation can alter photocatalytic behaviour by altering electronic structure, crystallinity, and surface properties, but the magnitude and direction of the effect remain system-dependent.

Compared with rare-earth doping, TM incorporation introduces 3d-derived electronic states and, for some dopants, variable oxidation states that can influence charge transfer and surface redox reactions. Rare-earth ions instead commonly modify the host through localized 4f states, defect chemistry, and changes in the local crystal environment. However, these mechanisms should not be treated as universally beneficial or mutually exclusive. For example, the Gd-doped ZnO study by Alasmari et al. associated the improved activity with defect-related charge trapping. In contrast, the Cu/Ni-doped ZnO study demonstrated that different TM dopants produced different kinetic responses within the same host system [50, 99]. Thus, the available evidence supports a system-dependent comparison rather than a general conclusion that either RE or TM doping provides superior photocatalytic performance.

Accordingly, meaningful comparison between RE- and TM-doped oxides should consider dopant concentration, host lattice, morphology, irradiation conditions, pollutant concentration, catalyst loading, and mechanistic evidence in addition to reported removal efficiency. This approach is more appropriate for identifying when a particular dopant strategy is advantageous and avoids attributing photocatalytic enhancement solely to the dopant class.

7.2 Benefits and Limitations of Transition-Metal Doping

TM doping can modify the optical and redox properties of metal oxide photocatalysts and, depending on the dopant and host lattice, can influence charge-carrier behaviour and photocatalytic activity [102]. However, these effects are concentration-dependent, and excessive incorporation may introduce defect states that favour charge recombination or alter the structural

properties of the host. Therefore, the benefits of TM incorporation must be evaluated for each specific dopant-host system rather than assumed to be universal.

Long-term stability is an additional consideration for practical application; a study investigated Ni-doped hematite and reported changes in photocatalytic and structural properties associated with Ni incorporation [103]. Such findings emphasize the need to evaluate structural retention and dopant stability during repeated operation rather than relying only on initial photocatalytic activity.

8. Metal Oxide Nanocomposites for Photocatalytic Dye Degradation

Metal oxide nanocomposites combine two or more functional components to overcome the limitations of individual photocatalysts. In photocatalytic dye degradation, coupling metal oxides or incorporating complementary phases can modify light absorption, interfacial charge transfer, surface reactivity, and other properties relevant to photocatalytic performance [76, 104]. These effects depend on the nature of the constituent phases and, particularly, on the quality of their interfaces.

Compared with rare-earth doping, which modifies a host oxide through dopant-induced changes in electronic structure, defect chemistry, and surface properties, nanocomposite formation relies mainly on interactions between distinct phases. Heterostructures can provide additional pathways for charge transfer, but the extent of enhancement depends on interfacial contact, phase composition, band alignment, morphology, and operating conditions. Nanocomposites are therefore considered here as a comparative modification strategy rather than as a universally superior alternative to rare-earth doping.

8.1 Structural and Photochemical Advantages

Nanocomposites can enhance photocatalytic performance by creating interfaces between distinct functional phases, thereby promoting charge separation, modifying charge-transfer pathways, and improving surface reactivity [105, 106]. Depending on the components and their electronic structures, these interfaces may form Type-II, Z-scheme, or Schottky configurations. However, the effectiveness of these configurations depends on interfacial contact, band alignment, phase composition, and morphology. Therefore, composite formation alone does not guarantee enhanced photocatalytic activity.

Recent studies emphasize that well-designed heterojunctions can improve charge separation, whereas unfavorable interfacial alignment or poor contact between phases may limit the expected benefit [104, 107]. Thus, the reported enhancement of nanocomposites should be interpreted in relation to their specific structural and reaction conditions rather than assumed to be universally superior to single oxides or other modification strategies.

8.2 Representative Nanocomposite Systems and Applications

Representative metal oxide nanocomposites reported for dye degradation are summarized in Table 2. The reported systems include graphene-based ZnO composites, mixed metal-oxide/rGO structures, magnetic Fe_3O_4@TiO_2-based composites, ZnO-TiO_2/rGO, NiO-SnO_2, and TiO_2-ZrO_2. These examples illustrate the different approaches used to combine complementary phases and modify photocatalytic behaviour under solar, visible, or UV irradiation.

Table 2 Representative metal oxide nanocomposites reported for photocatalytic dye degradation under UV, visible, or solar irradiation.

Nanocomposites	Dye	Time (min)	Degradation (%)	Light source	Initial dye conc. (mg/L)	Catalyst loading (mg/L)	Ref
GO-ZnO	MB	90	84	Sunlight	10	500	[108]
GO-ZnO-Ag	MB	40	100	Sunlight	10	500	[108]
GO-ZnO-Cu	MB	90	50	Sunlight	10	500	[108]
$CuO{\cdot}ZnO{\cdot}Fe_2O_3$/rGO	MB	80	87	UV-vis (200 W)	5	400	[109]
$CuO{\cdot}ZnO{\cdot}Fe_2O_3$	MB	80	77	UV-vis (200 W)	5	400	[109]
Fe_3O_4@TiO_2/Ag, Cu	RhB	90	86.19	Visible (500 W)	10	1000	[110]
ZnO-TiO_2/rGO	MB	63	99.7	UV (11 W)	20	252.5	[111]
NiO-SnO_2	BB	70	98	Sunlight	10	400	[112]
TiO_2-ZrO_2	AYGG	180	68	Sunlight	10	1000	[113]

The reported removal values vary substantially across the systems, but these values should not be used to establish a universal performance ranking because the studies were conducted using different dye concentrations, catalyst loadings, irradiation sources, and reaction times. Instead, Table 2 demonstrates that nanocomposite design can confer distinct functional advantages, including interfacial charge transfer, magnetic recovery, or improved activity under solar irradiation. Importantly, the available examples remain largely based on controlled laboratory conditions, limiting direct conclusions about their performance in real textile wastewater.

From the perspective of this review, these results support the role of nanocomposite formation as a complementary modification strategy to rare-earth doping rather than as a universally superior approach. Their practical advantage depends not only on photocatalytic activity but also on interface quality, recoverability, stability, and performance under realistic wastewater conditions.

8.3 Performance Limitations and Practical Challenges

Despite their potential advantages, nanocomposites face several challenges that may limit practical application. Achieving uniform interfacial contact and controlling aggregation are important for maintaining accessible active sites and effective charge transfer. In addition, catalyst recovery, long-term stability, and leaching require greater attention. The studies summarized in Table 2 were largely conducted under controlled laboratory conditions, and the available data are insufficient to establish how these materials would perform in real textile wastewater.

These limitations are important when comparing nanocomposites with rare-earth-doped oxides. Although interfacial engineering can provide additional pathways for charge transfer, nanocomposites may also introduce greater structural complexity and difficulties in synthesis, recovery, and long-term durability. Therefore, photocatalytic activity should be evaluated together with stability, recoverability, environmental safety, and performance under realistic wastewater conditions.

Future work should focus on controlled interface formation, extended cycling tests, quantitative leaching measurements, and validation using real wastewater. Standardized testing and life-cycle

assessment would also help determine whether the additional complexity of nanocomposite systems provides a meaningful practical advantage over simpler modification strategies [114-116].

9. Metal Oxide Core-Shell Nanostructures

Metal oxide core-shell nanostructures consist of a core material surrounded by a distinct shell, creating an interface between the two components. This architecture can provide control over surface properties, light response, and interfacial charge transfer, depending on the composition and structure of the core and shell [117]. In this review, core-shell systems are considered as a comparative modification strategy to illustrate how interfacial engineering differs from rare-earth doping.

Core-shell structures can be prepared by methods such as sol-gel coating, hydrothermal treatment, and Pechini synthesis. The preparation route influences shell thickness, crystallinity, morphology, and interfacial contact, thereby affecting the resulting photocatalytic behaviour. Representative systems and their reported operating conditions are summarized in Table 3.

Table 3 Representative metal oxide core-shell photocatalysts reported for dye degradation under UV, visible, or solar irradiation.

Core-shell photocatalyst	Dye	Time (min)	Light source	Initial dye conc. (mg/L)	Catalyst loading (mg/L)	Removal (%)	Ref.
ZnO/TiO_2	MB	20	Vis 575 W	50	1000	98	[118]
$TiO_2@SnO_2$	MB	180	UV 12 W	3.2	0.4	71	[119]
$ZnFe_2O_4@ZnO$	MO	240	UV 8 W	18.3	660	99	[120]
$ZnFe_2O_4@ZnO$	MO	240	Vis 125 W	18.3	660	62	[120]
SnO_2-$TiO_2/CoFe_2O_4$	RhB	90	UV 45 W	10	1000	100	[121]
SnO_2-$TiO_2/CoFe_2O_4$	RhB	120	Sunlight	10	1000	83.91	[121]
$NiFe_2O_4/ZnO$	Congo red	10	Simulated solar 350 W	20	1000	94.55	[122]
$CoFe_2O_4/ZnO$	Acid violet	100	UV 32 W	25	1000	76	[123]
$CoFe_2O_4/ZnO$	Acid brown	100	UV 32 W	25	1000	63	[123]
$(Co,Mn)Fe_2O_4@TiO_2$	RNL	960	UV 0.5-1 W	10	667	76.3	[124]
$NiFe_2O_4@TiO_2$	MO	NR	UV 300 W	8	800	90.06	[125]
ZnO:Ag	MB	90	UV-vis 100 W	10	429	96	[126]
ZnO:Ag	MO	120	UV-vis 100 W	10	429	86	[126]

9.1 Band Alignment and Interfacial Charge Transfer

The photocatalytic behaviour of a core-shell system depends on the electronic relationship between the two components and the quality of their interface. Appropriate band alignment can facilitate spatial separation of photogenerated charge carriers and reduce electron-hole recombination. However, the direction and extent of charge transfer are material-specific and should be determined from band positions and experimental evidence rather than assumed from the core-shell structure alone.

Experimental studies support this interface-dependent behaviour. For example, ZnO/TiO_2 core-shell structures showed reduced photoluminescence and increased photocurrent relative to the individual components, indicating improved charge separation. Excessive shell thickness, however, reduced the carrier density, demonstrating that the interface and shell structure must be optimized rather than increased [118]. Similar charge-carrier effects have been reported for TiO_2@SnO_2 core-shell nanoparticles [119].

9.2 Photocatalytic Performance and Practical Considerations

The systems summarized in Table 3 show substantial variation in reported dye removal. Still, these values should not be used to establish a direct performance ranking because the studies differ in dye concentration, catalyst loading, irradiation source, irradiation time, and other operating conditions. For example, $ZnFe_2O_4$@ZnO achieved 99% methyl orange removal after 240 min under UV irradiation, whereas ZnO/TiO_2 achieved 98% methylene blue removal after 20 min under visible irradiation [120]. These results illustrate the range of reported performance rather than demonstrating the superiority of one system over another.

Core-shell structures can also provide practical advantages such as magnetic separation and catalyst reuse. $NiFe_2O_4$/ZnO retained high dye-removal performance during repeated use, while the SnO_2-TiO_2/$CoFe_2O_4$ system was also evaluated over multiple cycles [121, 122]. Nevertheless, long-term structural stability, metal release, and performance in real textile wastewater remain less consistently evaluated than laboratory-scale dye removal. Thus, the core-shell architecture represents a useful interfacial design strategy, but its practical value should be assessed together with stability, recoverability, and realistic wastewater performance rather than removal efficiency alone.

10. Critical Discussion and Integrated Insights

Extensive research has demonstrated that metal oxide photocatalysts can effectively remove dyes under controlled laboratory conditions. Still, the evidence compiled in Sections 6-9 also reveals substantial variability in reported performance, mechanistic interpretation, and material design. Differences in catalyst composition, pollutant concentration, catalyst loading, irradiation conditions, reaction time, and wastewater matrix complicate the comparison. Therefore, the reported removal percentage should be interpreted within its experimental context rather than used alone to establish intrinsic photocatalyst superiority. The following discussion integrates these findings to identify the main factors that limit meaningful comparison and practical translation.

10.1 Comparative Interpretation of Modification Strategies

The comparison developed in Sections 6-9 does not identify a universally superior modification strategy. Rare-earth doping, transition-metal doping, nanocomposite formation, and core-shell architectures address different limitations of metal-oxide photocatalysts, including electronic-structure modification, defect engineering, interfacial charge transfer, and catalyst recovery [89, 98, 105]. However, the extent of these effects depends on the host material, modification level, morphology, interface quality, and reaction conditions.

Cross-study comparison is further limited by differences in catalyst loading, pollutant concentration, irradiation conditions, and reaction time [127]. These variables can substantially affect the measured photocatalytic response and should therefore be considered when interpreting the comparative data presented in Table 1, Table 2, and Table 3. Accordingly, the tables are intended to provide contextual comparisons rather than a ranking of intrinsic photocatalyst activity. Meaningful interpretation requires considering the reported removal efficiency together with catalyst loading, pollutant concentration, pH, irradiation conditions, reaction time, and kinetic information, while recognizing that missing or non-comparable parameters limit the strength of cross-study conclusions.

10.2 Mechanistic Confidence and Practical Reliability

A recurring limitation across the reviewed literature is the difference between observed photocatalytic performance and experimentally demonstrated mechanism. The revised RE-doped dataset illustrates this limitation: 15 of the 29 studies were classified as providing direct mechanistic evidence, whereas 14 provided only partial evidence. Similar caution is required for transition-metal-doped and heterostructured systems, where improved activity may be attributed to charge separation, defect formation, band-gap modification, or interfacial charge transfer without sufficient supporting measurements.

Mechanistic interpretation should therefore rely on complementary evidence, such as photoluminescence, electrochemical impedance spectroscopy, photocurrent measurements, ESR/EPR, scavenger experiments, or other spectroscopic analyses, rather than on degradation efficiency alone. The same evidence-based approach is needed when assessing practical reliability. Reuse, structural stability, catalyst loss, and metal or dopant release are reported less consistently than initial removal efficiency, limiting the assessment of long-term performance and environmental safety [114].

10.3 From Model Dyes to Real Wastewater

Most of the reviewed photocatalysts were evaluated using individual model dyes under controlled laboratory conditions. Such systems are useful for establishing photocatalytic behaviour, but they do not reproduce the chemical complexity of textile wastewater. Real effluents contain salts, surfactants, dissolved organic matter, suspended material, and competing pollutants that can affect adsorption, light penetration, and the availability of reactive species [128, 129].

In addition, dye removal or decolourization should not be interpreted as equivalent to complete mineralization or to reduced toxicity. Evidence of mineralization requires complementary measurements such as TOC or COD, while toxicity assessment requires appropriate analysis of degradation products or biological effects. This distinction is particularly important for azo dyes, for which cleavage of the chromophore may produce intermediate compounds that remain environmentally relevant [130].

For the RE-doped dataset analyzed here, the limitation is quantitative rather than merely qualitative: none of the 29 studies (0%) evaluated the catalyst using real wastewater, whereas all studies relied on controlled model-dye systems. Consequently, a direct numerical comparison of removal performance between model solutions and actual industrial effluents cannot be established for RE-doped photocatalysts from the available evidence. The absence of real-

wastewater testing also prevents assessment of how salinity, turbidity, dissolved organic matter, surfactants, suspended solids, and competing pollutants alter catalyst activity under application-relevant conditions. Future studies should therefore report model-solution and real-wastewater results under matched catalyst loading, irradiation conditions, reaction time, and analytical methods so that matrix effects can be quantified rather than inferred [129].

Overall, the evidence reviewed here indicates that the main value of material modification is not simply to obtain a higher dye-removal percentage, but to address specific limitations of the host photocatalyst while maintaining reproducible performance under realistic conditions. Rare-earth doping, transition-metal doping, nanocomposite formation, and core-shell architectures should therefore be viewed as complementary strategies whose suitability depends on material characteristics, pollutant chemistry, operating conditions, mechanistic confidence, stability, and wastewater complexity. This perspective provides the basis for the practical and research priorities discussed in the following sections.

Recent 2025 literature provides additional support for the broader conclusions of this review rather than fundamentally changing them. Recent work on ZnO-based photocatalysis and wastewater treatment continues to demonstrate the potential of modified metal oxides for pollutant removal, while recent discussion of rare-earth-doped ZnO further supports the role of rare-earth incorporation in modifying material properties and photocatalytic behaviour [24, 72, 131]. However, these recent studies do not address the limitations identified in the present analysis, particularly the dependence of reported performance on experimental conditions and the limited validation of mineralization, long-term stability, leaching, and real-wastewater performance. Thus, the newer evidence strengthens rather than reverses the central conclusion that RE doping is a promising modification strategy, but its practical superiority cannot be established from reported dye-removal efficiency alone.

11. Industrial and Practical Applicability of Metal Oxide Photocatalysis

High dye-removal efficiencies reported under laboratory conditions do not, by themselves, demonstrate industrial feasibility. Practical applications require the photocatalyst to maintain activity under complex wastewater conditions while meeting requirements for energy use, catalyst recovery, reactor operation, and treatment cost [132]. Thus, the relevant question is not whether metal oxide photocatalysts can achieve high removal in model solutions, but whether their performance remains adequate when these engineering and operational constraints are introduced.

Energy demand is a significant limitation, as many laboratory studies rely on artificial UV irradiation. The use of UV sources introduces an additional operating requirement that becomes increasingly important as treatment capacity increases [133]. Solar and visible-light-responsive photocatalysts can reduce dependence on artificial irradiation, and several modified metal oxides have demonstrated activity under solar or visible-light conditions [134, 135]. However, extending light absorption does not automatically establish practical superiority. Solar operation is affected by irradiation conditions and reactor configuration, making photon utilization and reactor design important factors in determining actual treatment performance [136]. Therefore, the benefit of visible-light activity should be evaluated at the process level rather than from the optical response of the catalyst alone.

Catalyst recovery represents a second practical constraint. Powdered nanoparticles provide high accessible surface area but are difficult to completely separate from treated water after operation [137]. Magnetic oxide-based materials offer one possible recovery strategy because the catalyst can be separated using an external magnetic field [138]. Immobilization can provide another route for catalyst retention, although it may alter mass transfer and the accessibility of active sites. Consequently, catalyst recoverability and activity retention should be considered together when assessing practical performance rather than treating recyclability as a secondary material property.

11.1 Performance in Real Industrial Wastewater

Most photocatalytic dye-degradation studies use single-dye solutions under controlled experimental conditions. Industrial textile wastewater is substantially more complex and may contain mixtures of dyes, surfactants, salts, and other dissolved or suspended constituents. Such components can alter adsorption, light penetration, and reactive-species availability, thereby altering photocatalytic performance relative to that observed in model solutions [128, 130].

The evidence compiled in this review demonstrates a major limitation in this area. None of the 29 RE-doped studies included in the present dataset reported photocatalytic testing using real wastewater. Consequently, the reported efficiencies cannot establish whether the apparent benefits of RE incorporation are retained in actual textile effluents. This evidence gap prevents reliable assessment of whether the reported benefits of RE incorporation would persist under the complex conditions of actual textile effluents. Real-wastewater validation should therefore be considered an essential criterion for establishing the practical significance of RE-doped photocatalysts. As an example of such application-oriented validation outside the RE-doped dataset, a recent study of Au-modified TiO_2 and ZnO evaluated photocatalytic degradation not only with model pollutants but also using untreated real textile wastewater [139].

The absence of real-wastewater validation is therefore a major limitation of the current RE-doped photocatalysis literature. While model dye solutions allow controlled assessment of catalyst activity, they do not reproduce the combined effects of salts, dissolved organic matter, surfactants, suspended solids, turbidity, and competing pollutants present in industrial effluents. Consequently, the reported laboratory efficiencies should be regarded as proof of photocatalytic potential rather than direct evidence of treatment performance under realistic wastewater conditions.

Industrial implementation also requires comparison with existing treatment processes, including adsorption, biological treatment, membrane separation, and other advanced oxidation processes. Such comparisons should consider energy demand, catalyst recovery, maintenance, treatment capacity, and overall process requirements rather than removal efficiency alone. Hybrid treatment configurations may provide a more realistic implementation strategy by assigning different treatment functions to complementary processes [129]. Thus, industrial applications may rely on process integration rather than complete replacement of conventional treatment. The major barriers to translating laboratory-scale photocatalytic dye treatment to industrial or field-scale applications are summarized in Figure 5.

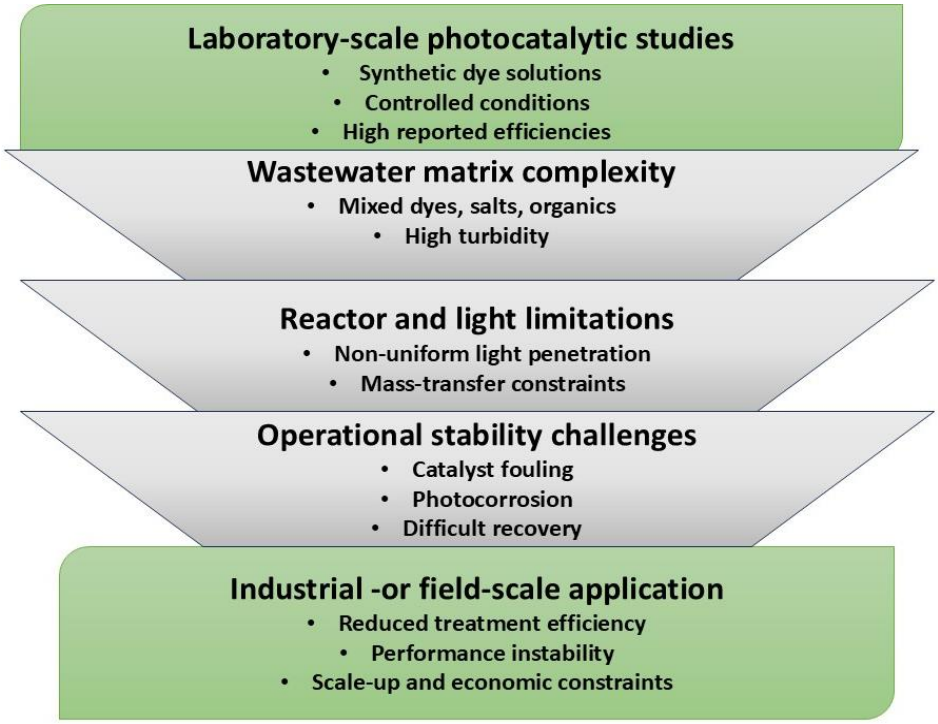

Figure 5 Key barriers to scaling up photocatalytic dye treatment.

11.2 Scale-Up Challenges and Reactor Engineering

The transition from laboratory reactors to industrial treatment introduces changes in irradiation, hydrodynamics, mass transfer, and catalyst utilization. Laboratory batch systems therefore cannot be directly extrapolated to continuous or larger-scale operation. Reactor design must balance catalyst concentration, hydraulic residence time, mixing, and photon utilization while limiting catalyst aggregation and light attenuation [140].

Reactor configuration is consequently a critical link between catalyst properties and treatment performance. Solar TiO_2 reactor systems have been specifically evaluated for reactor selection, scale-up, and commercialization [141], while photocatalytic membrane reactors provide another configuration for continuous water treatment. These studies demonstrate that reactor engineering must be considered alongside catalyst development when evaluating scale-up potential. However, reactor-level evidence remains insufficient to establish a standardized configuration for RE-doped photocatalysts.

11.3 Emerging Pilot Demonstrations and Industrial Case Studies

Pilot-scale studies provide a more relevant assessment of practical performance than conventional laboratory batch experiments. Immobilized TiO_2 has been evaluated in a pilot-scale wastewater-treatment reactor, demonstrating the feasibility of operating photocatalytic treatment beyond laboratory scale [142, 143]. Nevertheless, pilot demonstration alone does not establish commercial viability. Long-term activity retention, catalyst loss, energy consumption, treatment capacity, and treated-water quality must also be demonstrated under sustained operation.

Economic feasibility depends on the complete treatment process, including irradiation, catalyst preparation and replacement, recovery, reactor infrastructure, maintenance, and treatment

capacity. At present, the literature does not provide sufficiently standardized economic data to establish a reliable cost of treatment for RE-doped photocatalysts. A meaningful techno-economic assessment should therefore consider energy consumption, catalyst lifetime and replacement, recovery requirements, reactor and separation costs, treatment capacity, and operating and maintenance requirements using comparable treatment-based metrics. These factors should be evaluated alongside photocatalytic performance before claims of economic or commercial superiority are made [144].

Overall, the current evidence supports the technical potential of metal oxide photocatalysis but does not yet establish a clear industrial advantage for RE-doped systems. The principal gap is the lack of validation under real wastewater conditions, combined with incomplete evidence on reactor-scale performance and standardized economic assessment. Progress toward industrial application therefore requires a shift from reporting high removal efficiencies in model solutions toward demonstrating sustained performance under realistic wastewater and process conditions.

12. Future Research Directions

The evidence discussed in the preceding sections indicates that further progress in metal oxide photocatalysis requires a shift from material-centred optimization toward evidence-based and application-oriented research. The main unresolved issues concern mechanistic validation, standardized experimental reporting, real-wastewater performance, long-term stability and environmental safety, and translation from laboratory reactors to practical treatment systems. Accordingly, the following research priorities focus on strengthening the reliability of mechanistic conclusions, improving comparability across studies, and establishing the technical, environmental, and economic feasibility of promising photocatalytic systems.

12.1 Mechanistic and Experimental Challenges

A major priority is to strengthen the experimental basis for mechanistic interpretation. Many studies attribute enhanced photocatalytic activity to improved charge separation, oxygen-vacancy formation, or altered band structure, but provide insufficient spectroscopic, electrochemical, or kinetic evidence. Recent work has further shown that defect formation can either promote or hinder photocatalytic activity depending on defect type and concentration [145]. Future studies should therefore combine complementary techniques, including photoluminescence decay, transient absorption spectroscopy, electrochemical impedance spectroscopy, and carrier-lifetime measurements, to distinguish experimentally demonstrated charge-transfer processes from mechanisms inferred from removal efficiency alone.

Mechanistic validation should also move beyond post-reaction characterization. Operando or in situ spectroscopic and electrochemical measurements under irradiation and reaction conditions could provide more direct evidence of transient charge carriers, reactive intermediates, surface states, and interfacial charge-transfer pathways. Such measurements would reduce reliance on ex situ characterization and improve the reliability of mechanistic assignments.

A second priority is standardized experimental reporting. Photocatalytic performance is strongly affected by catalyst loading, initial dye concentration, pH, reaction volume, irradiation wavelength and intensity, reaction time, and reactor geometry, yet these parameters are not consistently reported [127]. This limits meaningful cross-study comparison and prevents reliable quantitative

synthesis. A minimum reporting framework should therefore include catalyst composition and loading, dye identity and concentration, pH, reaction volume, irradiation wavelength and measured irradiance where available, reaction time, kinetic constant, mineralization indicators such as TOC or COD, apparent quantum yield where measured, and catalyst recovery, reuse, and leaching data. Reporting these parameters would provide a more consistent basis for evaluating photocatalyst performance.

Real wastewater validation should be part of this framework. Textile effluents contain multiple dissolved and suspended constituents that can alter catalyst-pollutant interactions and reactive-species formation [146, 147]. Recent literature further emphasizes that catalyst behaviour can change substantially in the presence of competing pollutants and complex matrices [148]. For RE-doped photocatalysts, the present dataset contains no study using real wastewater; therefore, future investigations should prioritize actual textile effluents and report both pollutant removal and treatment-relevant outcomes such as mineralization, toxicity, stability, and energy consumption.

High-throughput experimentation and computational methods can complement these experimental approaches. AI- and machine-learning-assisted catalyst discovery could integrate composition, dopant concentration, structural descriptors, and reaction conditions to identify promising catalyst-wastewater combinations before experimental validation. Such approaches should be used to guide experimental design rather than replace mechanistic and experimental verification.

12.2 Material Stability, Environmental Safety, and Structural Optimization

Long-term stability remains insufficiently evaluated for many photocatalytic materials. ZnO photocorrosion, dopant leaching, and changes in catalyst structure during repeated use have been reported [149-151], but extended operation and quantitative release measurements remain uncommon. Future studies should therefore combine repeated-use experiments with post-reaction structural characterization and quantitative analysis of released metal or rare-earth species. Stability should be assessed under conditions that approximate the intended wastewater application rather than only under short laboratory cycles.

Environmental safety must also be evaluated alongside photocatalytic performance. Nanoparticles can generate reactive oxygen species and may interact with aquatic organisms after release [152]. Consequently, high dye-removal efficiency should not be interpreted as evidence of environmental safety. For RE-doped photocatalysts, the potential ecological effects of released rare-earth species also remain poorly characterized, particularly under repeated-use and realistic wastewater conditions. Future assessments should include ecotoxicity testing, nanoparticle release, dopant leaching, and, where appropriate, life-cycle assessment to evaluate environmental burdens associated with material synthesis, use, recovery, and disposal.

The optimum material structure is likewise unlikely to be universal across photocatalyst classes. Photocatalytic behaviour can depend on dopant concentration, interfacial architecture, morphology, and defect distribution, but the dominant factor varies among material systems [153, 154]. In particular, the relationship between dopant concentration and activity should be treated as system-specific rather than as a universal concentration window. High-throughput screening, computational modelling, and controlled defect engineering can help identify suitable structural

parameters for specific catalyst-pollutant systems, but predicted relationships should be confirmed experimentally.

12.3 Scale-Up, Process Integration, and Practical Implementation

Future research should shift from laboratory batch optimization toward controlled scale-up studies. Reactor hydrodynamics, light distribution, catalyst retention, mass transfer, and hydraulic residence time can substantially influence photocatalytic performance at larger scale [155]. Future pilot studies should therefore report these parameters, along with energy consumption, treated-water throughput, catalyst loading, and long-term activity so that laboratory and pilot-scale results can be compared on a process basis.

Process integration should also be investigated where photocatalysis alone is insufficient for complex wastewater treatment. Combining photocatalysis with adsorption, membrane separation, or biological treatment may allow individual processes to address complementary treatment requirements [156]. Such systems should be evaluated using overall treatment performance, energy demand, catalyst recovery, and process complexity rather than removal efficiency of the photocatalytic step alone.

Economic and environmental assessment should accompany scale-up. Techno-economic analysis should consider catalyst preparation and replacement, irradiation requirements, reactor operation, recovery, treatment capacity, and energy consumption. Life-cycle assessment should also evaluate material production, operational energy use, catalyst recovery, and end-of-life management. These assessments are necessary to determine whether improvements in photocatalytic activity translate into meaningful process-level advantages.

Overall, future development should follow an evidence-based pathway from mechanistic validation and standardized reporting to real-wastewater testing, long-term stability assessment, AI-assisted and experimentally verified material design, pilot-scale operation, and techno-economic and life-cycle evaluation. This progression would help shift photocatalytic research from isolated laboratory performance to reproducible, application-relevant wastewater treatment.

13. Conclusion

This review critically evaluated rare-earth-doped metal oxide photocatalysts for dye degradation by linking material modification with mechanistic evidence and practical treatment requirements. Across the 29 RE-doped studies examined, RE incorporation was associated with changes in optical, structural, morphological, and charge-carrier properties. Still, the available evidence does not support a single mechanism or material parameter as universally responsible for enhanced photocatalytic activity. In particular, oxygen-vacancy formation, 4f-related electronic states, and improved charge separation were frequently proposed, whereas direct experimental evidence for these mechanisms was less consistently available. Fifteen studies (51.7%) provided direct mechanistic evidence and 14 (48.3%) provided partial evidence, demonstrating that high reported removal does not necessarily correspond to strong mechanistic validation.

The analysis also shows that photocatalytic performance cannot be meaningfully ranked using dye-removal percentage alone. Differences in catalyst loading, dye concentration, pH, irradiation conditions, reaction time, morphology, and host structure substantially influence the reported response. The optimum RE concentration was likewise found to be system-specific rather than a

universal performance window. This evidence-based interpretation represents a central contribution of the review: the value of RE doping should be judged by the combination of material properties, mechanistic confidence, reaction conditions, and durability rather than by the highest reported removal percentage.

A major limitation of the present literature is the weak connection between model-solution performance and realistic wastewater treatment. None of the 29 RE-doped studies in the dataset reported photocatalytic testing using real wastewater. In addition, TOC analysis was reported in only 10 studies (34.5%), no study reported an apparent quantum yield, and quantitative leaching measurements were available in only one study. Stability or reuse testing was more common, being reported in 20 studies (69.0%), but long-term structural durability and dopant release remain insufficiently established. These limitations prevent reliable assessment of whether the reported benefits of RE incorporation can be maintained in complex industrial effluents.

The comparative analysis of transition-metal doping, nanocomposites, and core-shell architectures further indicates that no modification strategy is universally superior. The appropriate design depends on the host material, pollutant chemistry, operating conditions, mechanistic evidence, recoverability, stability, and wastewater matrix. The main advance provided by the present review is therefore a shift from efficiency-based comparison toward an evidence-based framework in which photocatalytic activity, mechanism, durability, and practical applicability are evaluated together.

Future research should follow a staged pathway. First, photocatalytic studies should adopt standardized reporting of catalyst composition and loading, dye concentration, pH, reaction volume, irradiation wavelength and measured intensity, reaction time, kinetic constants, mineralization, and catalyst reuse and leaching. Second, real textile wastewater should be incorporated into validation studies, together with TOC/COD, toxicity, stability, and energy-consumption measurements. Third, mechanistic claims should be supported by complementary characterization, including electrochemical, spectroscopic, and operando measurements where appropriate, rather than inferred from degradation efficiency alone. Fourth, AI-assisted and high-throughput approaches can be used to identify promising catalyst-pollutant combinations, but predictions should be experimentally validated. Finally, pilot-scale reactors, process integration, techno-economic analysis, and life-cycle assessment are needed to determine whether laboratory-scale improvements provide genuine environmental and process-level benefits. These priorities provide a practical path for advancing RE-doped photocatalysts from controlled laboratory studies toward reproducible and application-relevant wastewater treatment.

Acknowledgments

The authors would like to thank their institution for providing the necessary facilities to carry out this research.

Author Contributions

Adeeb Zaid: Conceptualization, methodology, investigation, data curation, formal analysis, writing-original draft. Prasenjit Maity: Supervision, validation, review and editing. Husam Al-Ziyadi: Review and editing. Jacob Wekalao: Review and editing. All authors have read and approved the final manuscript.

Funding

The authors received no financial support for the research, authorship, and/or publication of this article.

Data Availability Statement

The data supporting the findings of this study are available from the corresponding author upon reasonable request.

Competing Interests

The authors have declared that no competing interests exist.

AI-Assisted Technologies Statement

Artificial intelligence (AI) tools were used solely for language editing and grammar refinement during manuscript preparation. Specifically, OpenAI's ChatGPT was used to improve readability and linguistic clarity. All scientific concepts, literature analysis, interpretations, and conclusions were developed, verified, and approved by the authors. The authors accept full responsibility for the content of this manuscript.

Additional Materials

The following additional materials are uploaded at the page of this paper.

1. Table S1: Detailed experimental, characterization, and photocatalytic data for the RE-doped metal oxide catalysts.
2. Table S2: Comparison of the main synthesis routes represented in the reviewed rare-earth-doped metal oxide photocatalyst studies, including their principal advantages, limitations, and typical effects on morphology and structure.

References

1. Samsami S, Mohamadizaniani M, Sarrafzadeh MH, Rene ER, Firoozbahr M. Recent advances in the treatment of dye-containing wastewater from textile industries: Overview and perspectives. Process Saf Environ Prot. 2020; 143: 138-163.
2. Benkhaya S, M'rabet S, El Harfi A. A review on classifications, recent synthesis and applications of textile dyes. Inorg Chem Commun. 2020; 115: 107891.
3. Al-Tohamy R, Ali SS, Li F, Okasha KM, Mahmoud YA, Elsamahy T, et al. A critical review on the treatment of dye-containing wastewater: Ecotoxicological and health concerns of textile dyes and possible remediation approaches for environmental safety. Ecotoxicol Environ Saf. 2022; 231: 113160.
4. Slama HB, Chenari Bouket A, Pourhassan Z, Alenezi FN, Silini A, Cherif-Silini H, et al. Diversity of synthetic dyes from textile industries, discharge impacts and treatment methods. Appl Sci. 2021; 11: 6255.

5. Khan NA, Khan SU, Ahmed S, Farooqi IH, Yousefi M, Mohammadi AA, et al. Recent trends in disposal and treatment technologies of emerging-pollutants-a critical review. TrAC Trends Anal Chem. 2020; 122: 115744.
6. Wu H, Li L, Wang S, Zhu N, Li Z, Zhao L, et al. Recent advances of semiconductor photocatalysis for water pollutant treatment: Mechanisms, materials and applications. Phys Chem Chem Phys. 2023; 25: 25899-25924.
7. Naseem T, Durrani T. The role of some important metal oxide nanoparticles for wastewater and antibacterial applications: A review. Environ Chem Ecotoxicol. 2021; 3: 59-75.
8. Mohadesi M, Sanavi Fard M, Shokri A. The application of modified nano-TiO_2 photocatalyst for wastewater treatment: A review. Int J Environ Anal Chem. 2024; 104: 2571-2592.
9. Danish MS, Estrella LL, Alemaida IM, Lisin A, Moiseev N, Ahmadi M, et al. Photocatalytic applications of metal oxides for sustainable environmental remediation. Metals. 2021; 11: 80.
10. Ghamarpoor R, Fallah A, Jamshidi M. A review of synthesis methods, modifications, and mechanisms of ZnO/TiO_2-based photocatalysts for photodegradation of contaminants. ACS Omega. 2024; 9: 25457.
11. Siwińska-Stefańska K, Kubiak A, Piasecki A, Goscianska J, Nowaczyk G, Jurga S, et al. TiO_2-ZnO binary oxide systems: Comprehensive characterization and tests of photocatalytic activity. Materials. 2018; 11: 841.
12. Digbari Z, Monsef R, Salavati-Niasari M, Alsultany FH. $NiCrFeO_4$ nanostructures: Sonochemical synthesis, characterization and promising photocatalytic application for removal of toxic coloring agents under visible light. Results Eng. 2025; 26: 105096.
13. Mazaheri S, Monsef R, Alsultany FH, Salavati-Niasari M. Enhanced visible-light-driven photocatalytic potential of magnetic $NiMnFeO_4$/g-C_3N_4 nanocomposites for degradation of aqueous organic pollutants: Schiff-base ligand-assisted sol-gel auto-combustion synthesis, characterization and mechanism analysis. Appl Water Sci. 2025; 15: 130.
14. Salavati-Niasari M, Monsef R, Karami A, Aljeboree AM, Alsultany FH, Hamza HH. Sonochemical preparation and characterization of $ErVO_4$/g-C_3N_4 nano-photocatalysts for removal of water-soluble organic dyes under visible light exposures. Results Eng. 2025; 28: 107764.
15. El Mchaouri M, Mallah S, Abouhajjoub D, Boumya W, Elmoubarki R, Essadki A, et al. Engineering TiO_2 photocatalysts for enhanced visible-light activity in wastewater treatment applications. Tetrahedron Green Chem. 2025; 6: 100084.
16. Ngulube KF, Abdelhaleem A, Osman AI, Peng L, Nasr M. Advancing sustainable water treatment strategies: Harnessing magnetite-based photocatalysts and techno-economic analysis for enhanced wastewater management in the context of SDGs. Environ Sci Pollut Res. 2025; 32: 28159-28195.
17. Kumari H, Sonia, Suman, Ranga R, Chahal S, Devi S, et al. A review on photocatalysis used for wastewater treatment: Dye degradation. Water Air Soil Pollut. 2023; 234: 349.
18. Shaheen R, Alam N, Tahir K, Khan AU, Althagafi TM, Alabbosh KF, et al. Synergistic photocatalysis and bacterial inhibition by $ZrMg_2TiO_6$-$SeTiO_4$ nanocomposite: Insights into mechanisms and efficiency. Mater Chem Phys. 2025; 346: 131296.
19. Kamruzzaman M, Zapien JA, Rahman M, Afrose R, Anam TK, Liton MN, et al. Effects of p-type (Ag, Cu) dopant on the electronic, optical and photocatalytic properties of MoS_2, and impact on Au/Mo100-x-yAgxCuyS_2 performance. J Alloys Compd. 2021; 863: 158366.

20. Pratomo U, Fransisca N, Adzani MD, Irkham I, Sulaeman AP, Eddy DR, et al. Doping of rare earth element: The effects in elevated physical and optical properties of ZnO. Talanta Open. 2025; 11: 100411.
21. Zheng B, Fan J, Chen B, Qin X, Wang J, Wang F, et al. Rare-earth doping in nanostructured inorganic materials. Chem Rev. 2022; 122: 5519-5603.
22. Wei Y, Wang B, Ren R, Wang R. Effects of synthesis conditions on rare earth doped iron oxide catalyst for selective catalytic reduction of NOx with NH_3. Aerosol Air Qual Res. 2023; 23: 220438.
23. Sordello F, Berruti I, Gionco C, Paganini MC, Calza P, Minero C. Photocatalytic performances of rare earth element-doped zinc oxide toward pollutant abatement in water and wastewater. Appl Catal B Environ. 2019; 245: 159-166.
24. Sood S, Kumar P, Raina I, Misra M, Kaushal S, Gaur J, et al. Enhancing optoelectronic performance through rare-earth-doped ZnO: Insights and applications. Photonics. 2025; 12: 454.
25. Chen N, Liu B, Zhang P, Wang C, Du Y, Chang W, et al. Enhanced photocatalytic performance of Ce-doped SnO_2 hollow spheres by a one-pot hydrothermal method. Inorg Chem Commun. 2021; 132: 108848.
26. Ali Baig AB, Rathinam V, Palaninathan J. Facile synthesis of Ce-doped SnO_2 nanoparticles with enhanced performance for photocatalytic degradation of organic dye. J Iran Chem Soc. 2021; 18: 13-27.
27. Chahal S, Rani N, Kumar A, Kumar P. UV-irradiated photocatalytic performance of yttrium doped ceria for hazardous Rose Bengal dye. Appl Surf Sci. 2019; 493: 87-93.
28. Jian S, Tian Z, Zhang K, Duan G, Yang W, Jiang S. Hydrothermal synthesis of Ce-doped ZnO heterojunction supported on carbon nanofibers with high visible light photocatalytic activity. Chem Res Chin Univ. 2021; 37: 565-570.
29. Bandoh CK, Haruna M, Adu-Poku D, Danu BY, Pinto O, Toku M, et al. Gd-doped ZnO-g-C_3N_4 nanocomposite: A novel photocatalyst for the photodegradation of eosin yellow dye in water. Discov Appl Sci. 2025; 7: 272.
30. Khan U, Jan FA, Ullah R, Wajidullah, Ullah N, Salman. Comparative photocatalytic performance and therapeutic applications of zinc oxide (ZnO) and neodymium-doped zinc oxide (Nd-ZnO) nanocatalysts against Acid Yellow-3 dye: Kinetic and thermodynamic study of the reaction and effect of various parameters. J Mater Sci Mater Electron. 2022; 33: 2781-2800.
31. Verma V, Singh SV. La-doped TiO_2 nanoparticles for photocatalysis: Synthesis, activity in terms of degradation of methylene blue dye and regeneration of used nanoparticles. Arab J Sci Eng. 2023; 48: 16431-16443.
32. Yang DL, Feng QJ, Zhang R, Chen C, Wang JX. Efficient photocatalytic degradation of tetracycline using Yb-ZnO nanodispersion under visible light. J Water Process Eng. 2025; 79: 108985.
33. Akhtar J, Tahir MB, Sagir M, Bamufleh HS. Improved photocatalytic performance of Gd and Nd co-doped ZnO nanorods for the degradation of methylene blue. Ceram Int. 2020; 46: 11955-11961.
34. Bayan E, Volkova M, Tolstunov M, Chernyshev A. Synthesis of La-doped TiO_2 nanoparticles with enhanced photocatalytic activity. Nanotechnol Environ Eng. 2025; 10: 17.
35. Lal M, Sharma P, Ram C. Synthesis and photocatalytic potential of Nd-doped TiO_2 under UV and solar light irradiation using a sol-gel ultrasonication method. Results Mater. 2022; 15: 100308.

36. Hussaini AA, Unal F, Yıldırım M, Yıldız DE. Application of samarium doped zinc oxides nanocomposites in degradation of organic dye and antibiotic pollutants. Water Air Soil Pollut. 2026; 237: 1100.
37. Khan MM, Nain P, Kumar S, Ansari AA, Ahamed M, Shahabuddin M. Improved photocatalytic and electrochemical activities of (Nd^{3+}, Yb^{3+}) co-doped TiO_2 nanoparticles synthesized by hydrothermal protocol. J Mater Sci Mater Electron. 2024; 35: 2149.
38. Pascariu P, Cojocaru C, Samoila P, Romanitan C. Nd-doped ZnO nanostructures with enhanced photocatalytic performance for environmental protection. Int J Mol Sci. 2023; 24: 6436.
39. Anwar M, Kayani ZN, Hassan A, Zeeshan T, Riaz S, Naseem S. Enhancement in photocatalytic activity and biological properties of Sm doped ZnO nanostructures by the increase in Sm contents. Inorg Chem Commun. 2023; 158: 111431.
40. Dhanraj G, Raina O, Surendar M, Gopinath S, Manthrammel MA, Shkir M. Stable and cost-effective La-doped WO_3 nanoparticles for photocatalytic degradation of organic and antibiotic pollutants under visible light. Ceram Int. 2025; 51: 15030-15042.
41. Raina I, Kumar P, Kumar A, Singh K, Somvanshi A, Soni R, et al. Visible-light activated La-doped ZnO photocatalysts for enhanced degradation of crystal violet dye. Ceram Int. 2025; 51: 54185-54199.
42. Selvaraj S, Vangari GA, Mohan MK. Facile synthesis of Sm doped ZnO nanoflowers by Co-precipitation method for enhanced photocatalytic degradation of MB dye under sunlight irradiation. Ceram Int. 2022; 48: 29049-29058.
43. Choudhary K, Saini R, Purohit LP. Controllable synthesis of Ce-doped ZnO: TiO_2 nanospheres for photocatalytic degradation of MB dye and levofloxacin under sunlight light irradiation. Opt Mater. 2023; 143: 114167.
44. Mao T, Wang W, Liu P, Zha J, Bu X, Song R, et al. Sol-Gel synthesis of Yb-Er Co-doped TiO_2-ZnO heterostructures for enhanced photocatalytic degradation of methylene blue: Performance and mechanism. J Mater Sci Mater Electron. 2026; 37: 1145.
45. Silva MCR, Castro-Lopes S, Jerônimo AG, Barbosa R, Lins A, Trigueiro P, et al. Green synthesis of Er-doped ZnO nanoparticles: An investigation on the methylene blue, eosin, and ibuprofen removal by photodegradation. Molecules. 2024; 29: 391.
46. Sargunavathi S, Balamurugan S, Avula B, Abisheik T, Kumar NL, Pandiyan V, et al. Rare-earth (Er^{3+}) modified ZnO photocatalyst: Dual action in organic dye degradation under UV/solar light and microbial suppression. J Water Process Eng. 2026; 81: 109188.
47. Rajeev YN, Magdalane CM, Hepsibha S, Ramalingam G, Kumar BA, Kumar LB, et al. Europium decorated hierarchical TiO_2 heterojunction nanostructure with enhanced UV light photocatalytic activity for degradation of toxic industrial effluent. Inorg Chem Commun. 2023; 157: 111339.
48. Hamdi D, Mansouri L, Srivastava V, Sillanpaa M, Bousselmi L. Cerium and europium doped TiO_2 thin films deposited by a sol-gel dip-coating process: Characterization and photocatalytic activity toward dye degradation. Turk J Chem. 2022; 46: 415-433.
49. Yu X, Sa G, Xu A. Effective removal of quinoline in wastewater using Gd-TiO_2 photocatalyst. Vacuum. 2025; 246: 115019.
50. Alasmari A, Alresheedi NM, Alzahrani MA, Aldosari FM, Ghasemi M, Ismail A, et al. High-performance photocatalytic degradation-a ZnO nanocomposite co-doped with Gd: A systematic study. Catalysts. 2024; 14: 946.

51. Keerthana SP, Yuvakkumar R, Kumar PS, Ravi G, Velauthapillai D. Nd doped ZrO_2 photocatalyst for organic pollutants degradation in wastewater. Environ Technol Innov. 2022; 28: 102851.
52. Mahmoud ZH, AL-Bayati RA, Khadom AA. The efficacy of samarium loaded titanium dioxide (Sm: TiO_2) for enhanced photocatalytic removal of rhodamine B dye in natural sunlight exposure. J Mol Struct. 2022; 1253: 132267.
53. Nain P, Pawar M, Rani S, Kumar S, Khan MM. (Ho, Yb) co-doping effects on structural, optical, photocatalytic and thermal properties of TiO_2 NPs prepared by hydrothermal approach. Physica B. 2025; 706: 417132.
54. Roy M, Saha R. Dyes and their removal technologies from wastewater: A critical review. In: Intelligent environmental data monitoring for pollution management. New York, NY: Academic Press; 2021. pp. 127-160.
55. Manavi N, Kazemi AS, Bonakdarpour B. The development of aerobic granules from conventional activated sludge under anaerobic-aerobic cycles and their adaptation for treatment of dyeing wastewater. Chem Eng J. 2017; 312: 375-384.
56. Laothanachareon T, Kongtong K, Saeng-Kla K, Kanokratana P, Leetanasaksakul K, Champreda V. Evaluating the efficacy of wood decay fungi and synthetic fungal consortia for simultaneous decolorization of multiple textile dyes. World J Microbiol Biotechnol. 2023; 39: 226.
57. Mohamadpour F, Amani AM. Photocatalytic systems: Reactions, mechanism, and applications. RSC Adv. 2024; 14: 20609-20645.
58. Mathew S, John BK, Abraham T, Mathew B. Metal-doped titanium dioxide for environmental remediation, hydrogen evolution and sensing: A review. ChemistrySelect. 2021; 6: 12742-12751.
59. Dutta P, Rabbi MD, Sufian M, Mahjebin S. Effects of textile dyeing effluent on the environment and its treatment: A review. Eng Appl Sci Lett. 2022; 5: 1-17.
60. AlMohamadi H, Awad SA, Sharma AK, Fayzullaev N, Távara-Aponte A, Chiguala-Contreras L, et al. Photocatalytic activity of metal-and non-metal-anchored ZnO and TiO_2 nanocatalysts for advanced photocatalysis: Comparative study. Catalysts. 2024; 14: 420.
61. Liu C, Xu C, Wang W, Chen L, Li X, Wu Y. Oxygen vacancy mediated band-gap engineering via B-doping for enhancing Z-scheme A-TiO_2/R-TiO_2 heterojunction photocatalytic performance. Nanomaterials. 2023; 13: 794.
62. Suman, Chahal S, Kumar A, Kumar P. Zn doped α-Fe_2O_3: An efficient material for UV driven photocatalysis and electrical conductivity. Crystals. 2020; 10: 273.
63. Wang Z, Gong C, Zhang C, Zhao C, Su TS, Li H, et al. Recent advances in interfacial engineering for high-efficiency perovskite photovoltaics. DeCarbon. 2025; 8: 100107.
64. Aragaw TA. A review of dye biodegradation in textile wastewater, challenges due to wastewater characteristics, and the potential of alkaliphiles. J Hazard Mater Adv. 2024; 16: 100493.
65. Pavel M, Anastasescu C, State RN, Vasile A, Papa F, Balint I. Photocatalytic degradation of organic and inorganic pollutants to harmless end products: Assessment of practical application potential for water and air cleaning. Catalysts. 2023; 13: 380.
66. Flores Alarcón MA, Pacheco CR, Bustos KG, Meza KT, Terán-Hilares F, Tanaka DavidAP, et al. Efficient dye removal from real textile wastewater using orange seed powder as suitable bio-adsorbent and membrane technology. Water. 2022; 14: 4104.
67. Raizada P, Soni V, Kumar A, Singh P, Khan AA, Asiri AM, et al. Surface defect engineering of metal oxides photocatalyst for energy application and water treatment. J Materiomics. 2021; 7: 388-418.

68. Hassaan MA, El-Nemr MA, Elkatory MR, Ragab S, Niculescu VC, El Nemr A. Principles of photocatalysts and their different applications: A review. Top Curr Chem. 2023; 381: 31.
69. Kocijan M, Podlogar M. Perspective chapter: Modification engineering of titanium dioxide-based nanostructured photocatalysts for efficient removal of pollutants from water. Titanium Dioxide-Uses, Applications, and Advances. London, UK: IntechOpen; 2024.
70. Pérez-Lucas G, El Aatik A, Aliste M, Hernández V, Fenoll J, Navarro S. Reclamation of aqueous waste solutions polluted with pharmaceutical and pesticide residues by biological-photocatalytic (solar) coupling in situ for agricultural reuse. Chem Eng J. 2022; 448: 137616.
71. Ye Z, Xu Z, Yue W, Liu X, Wang L, Zhang J. Exploiting the LSPR effect for an enhanced photocatalytic hydrogen evolution reaction. Phys Chem Chem Phys. 2023; 25: 2706-2716.
72. Kaur N, Bansal M, Kaur P, Kaur K, Awasthi A, Nippani SK, et al. Mitigating dye and organic pollutant-driven surface water pollution using ZnO nanoparticles: A sustainable strategy for climate resilience. Front Environ Sci. 2025; 13: 1656031.
73. Fdez-Sanromán A, Pazos M, de Vasconcelos Lanza MR, Garcia-Segura S, Dória AR. Toward the treatment of bisphenol F in real water matrices: Assessing the potential of electrochemically-driven UVC/e-H_2O_2. Appl Catal O Open. 2026; 218: 207109.
74. Ishchenko OM, Rogé V, Lamblin G, Lenoble D. TiO_2-and ZnO-based materials for photocatalysis: Material properties, device architecture and emerging concepts. Semiconductor photocatalysis-materials, mechanisms and applications. London, UK: IntechOpen; 2016.
75. Eddy DR, Permana MD, Sakti LK, Sheha GA, Solihudin, Hidayat S, et al. Heterophase polymorph of TiO_2 (Anatase, Rutile, Brookite, TiO_2 (B)) for efficient photocatalyst: Fabrication and activity. Nanomaterials. 2023; 13: 704.
76. Theerthagiri J, Chandrasekaran S, Salla S, Elakkiya V, Senthil RA, Nithyadharseni P, et al. Recent developments of metal oxide based heterostructures for photocatalytic applications towards environmental remediation. J Solid State Chem. 2018; 267: 35-52.
77. Alsulmi A, Mohamed K, Mohammed NN, Rabee MM, Soltan A, Messih MA, et al. Sonochemical synthesis of S-scheme CuO/CeO_2 heterojunction for enhanced photocatalytic degradation of rhodamine B dye under solar radiations. Ceram Int. 2024; 50: 36349-36362.
78. Cui T, Su Y, Fu X, Zhu Y, Zhang Y. The key role of surface hydroxyls on the activity and selectivity in photocatalytic degradation of organic pollutants and NO removal. J Alloys Compd. 2022; 921: 165931.
79. Zaid A, Al-Ziyadi H, Dave P, Maity P. Morphology-engineered ZnO tetrapods for rapid UV-driven photocatalytic degradation of methylene blue: Statistical optimization and mechanistic insights. Nano Struct Nano Obj. 2026; 47: 101733.
80. Reshma R, James C, Sasi BA, Jolly SS, Twinkle AR. Oxygen vacancy-engineered $Ti_3C_2T_x$ MXenes for photocatalytic degradation of pharmaceutical residues in aqueous systems: Molecular mechanisms and future directions. Next Mater. 2025; 9: 101127.
81. Zhang Q, Zhao X, Duan L, Shen H, Liu R. Controlling oxygen vacancies and enhanced visible light photocatalysis of CeO_2/ZnO nanocomposites. J Photochem Photobiol A Chem. 2020; 392: 112156.
82. Tuc Altaf C, Colak TO, Rostas AM, Popa A, Toloman D, Suciu M, et al. Impact on the photocatalytic dye degradation of morphology and annealing-induced defects in zinc oxide nanostructures. ACS Omega. 2023; 8: 14952-14964.

83. Rajput RB, Jamble SN, Kale RB. A review on TiO_2/SnO_2 heterostructures as a photocatalyst for the degradation of dyes and organic pollutants. J Environ Manage. 2022; 307: 114533.
84. Apostolova I, Apostolov A, Wesselinowa J. Band gap tuning in transition metal and rare-earth-ion-doped TiO_2, CeO_2, and SnO_2 nanoparticles. Nanomaterials. 2022; 13: 145.
85. Varaprasad HS, Sridevi PV, Anuradha MS. Optical, morphological, electrical properties of ZnO-TiO_2-SnO_2/CeO_2 semiconducting ternary nanocomposite. Adv Powder Technol. 2021; 32: 1472-1480.
86. Djurišić AB, Leung YH, Ching Ng AM. Strategies for improving the efficiency of semiconductor metal oxide photocatalysis. Mater Horiz. 2014; 1: 400-410.
87. Zeid SA, Leprince-Wang Y. Advancements in ZnO-based photocatalysts for water treatment: A comprehensive review. Crystals. 2024; 14: 611.
88. Kannan P, Maduraiveeran G. Metal oxides nanomaterials and nanocomposite-based electrochemical sensors for healthcare applications. Biosensors. 2023; 13: 542.
89. An J, Qu Y, Wang G. The multiple roles of rare earth elements in the field of photocatalysis. Inorg Chem Front. 2023; 11: 11-28.
90. Habib IY, Zain NM, Lim CM, Usman A, Kumara NT, Mahadi AH. Effect of doping rare-earth element on the structural, morphological, optical and photocatalytic properties of ZnO nanoparticles in the degradation of methylene blue dye. IOP Conf Ser Mater Sci Eng. 2021; 1127: 012004.
91. Sarkar A, Eggert B, Velasco L, Mu X, Lill J, Ollefs K, et al. Role of intermediate 4f states in tuning the band structure of high entropy oxides. APL Mater. 2020; 8: 051111.
92. Wen C, Ni X, Han M, Yu Y, Liu C, Zhang Y, et al. The function of photocatalytic performance and carrier separation efficiency tuned by doping content in homogeneous photocatalysts. Adv Sci. 2025; 12: 2501026.
93. Basumatary B, Basumatary R, Ramchiary A, Konwar D. Evaluation of Ag@TiO_2/WO_3 heterojunction photocatalyst for enhanced photocatalytic activity towards methylene blue degradation. Chemosphere. 2022; 286: 131848.
94. Kaneva N, Bojinova A, Papazova K. Enhanced removal of organic dyes using co-catalytic Ag-modified ZnO and TiO_2 sol-gel photocatalysts. Catalysts. 2023; 13: 245.
95. Ishchenko O, Rogé V, Lamblin G, Lenoble D, Fechete I. TiO_2, ZnO, and SnO_2-based metal oxides for photocatalytic applications: Principles and development. C R Chimie. 2021; 24: 103-124.
96. Krishnan A, Swarnalal A, Das D, Krishnan M, Saji VS, Shibli SM. A review on transition metal oxides based photocatalysts for degradation of synthetic organic pollutants. J Environ Sci. 2024; 139: 389-417.
97. Ahmed TY, Abdullah OG, Mamand SM, Aziz SB. Band structure study of pure and doped anatase titanium dioxide (TiO_2) using first-principle-calculations: Role of atomic mass of transition metal elements (TME) on band gap reduction. Opt Quantum Electron. 2024; 56: 1249.
98. Sharma M, Sajwan D, Gouda A, Sharma A, Krishnan V. Recent progress in defect-engineered metal oxides for photocatalytic environmental remediation. Photochem Photobiol. 2024; 100: 830-896.
99. Al-Mamun MR, Rokon MZ, Rahim MA, Hossain MI, Islam MS, Ali MR, et al. Enhanced photocatalytic activity of Cu and Ni-doped ZnO nanostructures: A comparative study of methyl orange dye degradation in aqueous solution. Heliyon. 2023; 9: e16506.

100. Mehmood F, Iqbal J, Ismail M, Mehmood A. Ni doped WO_3 nanoplates: An excellent photocatalyst and novel nanomaterial for enhanced anticancer activities. J Alloys Compd. 2018; 746: 729-738.
101. Reddy CV, Reddy IN, Ravindranadh K, Reddy KR, Kim D, Shim J. Ni-dopant concentration effect of ZrO_2 photocatalyst on photoelectrochemical water splitting and efficient removal of toxic organic pollutants. Sep Purif Technol. 2020; 252: 117352.
102. Santos E, Catto AC, Peterline AF, Avansi Jr W. Transition metal (Nb and W) doped TiO_2 nanostructures: The role of metal doping in their photocatalytic activity and ozone gas-sensing performance. Appl Surf Sci. 2022; 579: 152146.
103. Chahal S, Singh S, Goel P, Kumar A, Singh O, Kumar P. Understanding the role of Ni ions on the photocatalytic activity and dielectric properties of hematite nanostructures: An experimental and DFT approach. J Phys Chem Solids. 2021; 156: 110118.
104. Mushtaq N, Ahmad A, Erum JK, Li L, Qian J, Wang X, et al. Shaping the future of solar-driven photocatalysis by reticular framework materials. J Mater Sci Technol. 2025; 231: 193-244.
105. Gerasimov E. Synthesis of nanocomposites and catalysis applications II. Nanomaterials. 2023; 13: 3054.
106. Wakjira TL, Gemta AB, Kassahun GB, Andoshe DM, Tadele K. Bismuth-based Z-scheme heterojunction photocatalysts for remediation of contaminated water. ACS Omega. 2024; 9: 8709-8729.
107. Samarasinghe LV, Muthukumaran S, Baskaran K. Heterojunction photocatalysts for solar-driven wastewater treatment: Interfacial design, charge carrier dynamics, and advanced characterization techniques. J Water Process Eng. 2025; 79: 108960.
108. Al-Rawashdeh NA, Allabadi O, Aljarrah MT. Photocatalytic activity of graphene oxide/zinc oxide nanocomposites with embedded metal nanoparticles for the degradation of organic dyes. ACS Omega. 2020; 5: 28046-28055.
109. Fatima R, Warsi MF, Zulfiqar S, Ragab SA, Shakir I, Sarwar MI. Nanocrystalline transition metal oxides and their composites with reduced graphene oxide and carbon nanotubes for photocatalytic applications. Ceram Int. 2020; 46: 16480-16492.
110. Dehghani M, Rashidizadeh A, Ghafuri H, Rabbani M. Synthesis and characterization of magnetic nanocomposite Fe_3O_4@TiO_2/Ag, Cu and investigation of photocatalytic activity by degradation of rhodamine B (RhB) under visible light irradiation. Optik. 2019; 179: 646-653.
111. Viet TQ, Khoi VH, Giang NT, Van Anh HT, Dat NM, Phong MT, et al. Statistical screening and optimization of photocatalytic degradation of methylene blue by ZnO-TiO_2/rGO nanocomposite. Colloids Surf A. 2021; 629: 127464.
112. Begum S, Mishra SR, Ahmaruzzaman M. Facile synthesis of NiO-SnO_2 nanocomposite for enhanced photocatalytic degradation of bismarck brown. Inorg Chem Commun. 2022; 143: 109721.
113. Ramamoorthy S, Das S, Balan R, Lekshmi IC. TiO_2-ZrO_2 nanocomposite with tetragonal zirconia phase and photocatalytic degradation of Alizarin Yellow GG azo dye under natural sunlight. Mater Today Proc. 2021; 47: 4641-4646.
114. Beil SB, Bonnet S, Casadevall C, Detz RJ, Eisenreich F, Glover SD, et al. Challenges and future perspectives in photocatalysis: Conclusions from an interdisciplinary workshop. JACS Au. 2024; 4: 2746-2766.

115. Nizam NU, Hanafiah MM, Woon KS. A content review of life cycle assessment of nanomaterials: Current practices, challenges, and future prospects. Nanomaterials. 2021; 11: 3324.
116. Gottardo S, Mech A, Drbohlavová J, Małyska A, Bøwadt S, Sintes JR, et al. Towards safe and sustainable innovation in nanotechnology: State-of-play for smart nanomaterials. NanoImpact. 2021; 21: 100297.
117. Huseien GF. Potential applications of core-shell nanoparticles in construction industry revisited. Appl Nano. 2023; 4: 75-114.
118. Mehr ME, Maleki-Ghaleh H, Yarahmadi M, Kavanlouei M, Siadati MH. Synthesis and characterization of photocatalytic zinc oxide/titanium oxide (core/shell) nanocomposites. J Alloys Compd. 2021; 882: 160777.
119. Farhadi A, Mohammadi MR, Ghorbani M. On the assessment of photocatalytic activity and charge carrier mechanism of TiO_2@SnO_2 core-shell nanoparticles for water decontamination. J Photochem Photobiol A Chem. 2017; 338: 171-177.
120. Kulkarni SD, Kumbar S, Menon SG, Choudhari KS. Magnetically separable core-shell $ZnFe_2O_4$@ZnO nanoparticles for visible light photodegradation of methyl orange. Mater Res Bull. 2016; 77: 70-77.
121. Huang J, Jing HX, Li N, Li LX, Jiao WZ. Fabrication of magnetically recyclable SnO_2-TiO_2/$CoFe_2O_4$ hollow core-shell photocatalyst: Improving photocatalytic efficiency under visible light irradiation. J Solid State Chem. 2019; 271: 103-109.
122. Zhu HY, Jiang R, Fu YQ, Li RR, Yao J, Jiang ST. Novel multifunctional $NiFe_2O_4$/ZnO hybrids for dye removal by adsorption, photocatalysis and magnetic separation. Appl Surf Sci. 2016; 369: 1-10.
123. Ferdosi E, Bahiraei H, Ghanbari D. Investigation the photocatalytic activity of $CoFe_2O_4$/ZnO and $CoFe_2O_4$/ZnO/Ag nanocomposites for purification of dye pollutants. Sep Purif Technol. 2019; 211: 35-39.
124. Neris AM, Schreiner WH, Salvador C, Silva UC, Chesman C, Longo E, et al. Photocatalytic evaluation of the magnetic core@shell system (Co, Mn) Fe_2O_4@TiO_2 obtained by the modified Pechini method. Mater Sci Eng B. 2018; 229: 218-226.
125. Baig MM, Pervaiz E, Afzal MJ. Catalytic activity and kinetic studies of core@shell nanostructure $NiFe_2O_4$@TiO_2 for photocatalytic degradation of methyl orange dye. J Chem Soc Pak. 2020; 42: 531-541.
126. Jadhav J, Biswas S. Hybrid ZnO: Ag core-shell nanoparticles for wastewater treatment: Growth mechanism and plasmonically enhanced photocatalytic activity. Appl Surf Sci. 2018; 456: 49-58.
127. Groeneveld I, Kanelli M, Ariese F, van Bommel MR. Parameters that affect the photodegradation of dyes and pigments in solution and on substrate-an overview. Dyes Pigm. 2023; 210: 110999.
128. Rashid TU, Kabir SF, Biswas MC, Bhuiyan MR. Sustainable wastewater treatment via dye-surfactant interaction: A critical review. Ind Eng Chem Res. 2020; 59: 9719-9745.
129. Bissenova M, Idrissov N, Kuspanov Z, Umirzakov A, Daulbayev C. Hybrid adsorption-photocatalysis composites: A sustainable route for efficient water purification. Mater Renew Sustain Energy. 2025; 14: 44.
130. Muscetta M, Ganguly P, Clarizia L. Solar-powered photocatalysis in water purification: Applications and commercialization challenges. J Environ Chem Eng. 2024; 12: 113073.

131. Chalatsi-Diamanti P, Isari EA, Grilla E, Kokkinos P, Kalavrouziotis IK. Recent prospects, challenges and advancements of photocatalysis as a wastewater treatment method. Water Emerg. Contam. Nanoplastics. 2025; 4: 12.
132. Shukla S, Pandey H, Singh P, Tiwari AK, Baranwal V, Pandey AC. Synergistic impact of photocatalyst and dopants on pharmaceutical-polluted waste water treatment: A review. Environ Pollut Bioavailab. 2021; 33: 347-364.
133. Zhi J. Prospects and challenges analysis of UV led technology in practical applications. Highlights Sci Eng Technol. 2024; 121: 90-97.
134. Khlifi N, Zerrouki C, Fourati N, Guermazi H, Guermazi S. Investigation of structural and optical properties of TM-doped CuO NPs: Correlation with their photocatalytic efficiency in sunlight-induced pollutant degradation. Measurement. 2024; 237: 115209.
135. Mohapatra L, Parida K. A review of solar and visible light active oxo-bridged materials for energy and environment. Catal Sci Technol. 2017; 7: 2153-2164.
136. Degerli SN, Gramegna A, Tommasi M, Ramis G, Rossetti I. Reactor and plant designs for the solar photosynthesis of fuels. Energies. 2024; 17: 3112.
137. Khdair AI, Aburumman GA, Gholipour S, Afrand M. Nanoparticles in water purification: Multifunctional roles, challenges, and sustainable applications. Environ Sci Nano. 2025; 12: 3871-3895.
138. Krishnan Y, Babu K, Sakkaraiyan S, Dinesh A, Shanmugam A, Radhakrishnan K, et al. Spinel cobalt ferrite nanoparticles for photocatalysts, sensor and biomedical applications: A review. Semiconductors. 2024; 58: 721-739.
139. Zaid A, Yaou Balarabe B, Maity P. Gold plasmon-enhanced TiO_2 and ZnO nanocomposites for rapid photodegradation of dyes, pharmaceuticals, and real textile wastewater. Sci Rep. 2026. doi: 10.1038/s41598-026-65244-7.
140. Towler G, Sinnott R. Chapter 15-Design of reactors and mixers. In: Chemical Engineering Design. 3rd ed. Oxford, UK: Butterworth-Heinemann; 2022. pp. 497-588.
141. Molinari R, Severino A, Lavorato C, Argurio P. Which configuration of photocatalytic membrane reactors has a major potential to be used at an industrial level in tertiary sewage wastewater treatment? Catalysts. 2023; 13: 1204.
142. Abdel-Maksoud Y, Imam E, Ramadan A. TiO_2 solar photocatalytic reactor systems: Selection of reactor design for scale-up and commercialization-analytical review. Catalysts. 2016; 6: 138.
143. Kane A, Assadi AA, El Jery A, Badawi AK, Kenfoud H, Baaloudj O, et al. Advanced photocatalytic treatment of wastewater using immobilized titanium dioxide as a photocatalyst in a pilot-scale reactor: Process intensification. Materials. 2022; 15: 4547.
144. Chai SY, Phang FJ, Yeo LS, Ngu LH, How BS. Future era of techno-economic analysis: Insights from review. Front Sustain. 2022; 3: 924047.
145. Ali H, Ajmal Z, Alzahrani AY, Al Mughram MH, Abu-Dief AM, Al-Faze R, et al. Defect-driven innovations in photocatalysts: Pathways to enhanced photocatalytic applications. InfoMat. 2025; 7: e70040.
146. Periyasamy AP. Recent advances in the remediation of textile-dye-containing wastewater: Prioritizing human health and sustainable wastewater treatment. Sustainability. 2024; 16: 495.
147. Azanaw A, Birlie B, Teshome B, Jemberie M. Textile effluent treatment methods and eco-friendly resolution of textile wastewater. Case Stud Chem Environ Eng. 2022; 6: 100230.

148. Shi C, Jia Y, Zhang X, Wang T, Li J, Qian J, et al. The interaction between pollutants and catalysts: From fundamentals to its application in heterogeneous fenton-like systems. ACS ES T Water. 2025; 5: 2778-2792.
149. Velmurugan R, Selvam K, Krishnakumar B, Swaminathan M. An efficient reusable and antiphotocorrosive nano ZnO for the mineralization of Reactive Orange 4 under UV-A light. Sep Purif Technol. 2011; 80: 119-124.
150. Warren Z, Wenk J, Mattia D. Increased photocorrosion resistance of ZnO foams via transition metal doping. RSC Adv. 2023; 13: 2438-2450.
151. Mirzaeifard Z, Shariatinia Z, Jourshabani M, Rezaei Darvishi SM. ZnO photocatalyst revisited: Effective photocatalytic degradation of emerging contaminants using S-doped ZnO nanoparticles under visible light radiation. Ind Eng Chem Res. 2020; 59: 15894-15911.
152. Fu PP, Xia Q, Hwang HM, Ray PC, Yu H. Mechanisms of nanotoxicity: Generation of reactive oxygen species. J Food Drug Anal. 2014; 22: 64-75.
153. Mutuma BK, Mathebula X, Nongwe I, Mtolo BP, Matsoso BJ, Erasmus R, et al. Unravelling the interfacial interaction in mesoporous SiO_2@nickel phyllosilicate/TiO_2 core-shell nanostructures for photocatalytic activity. Beilstein J Nanotechnol. 2020; 11: 1834-1846.
154. Rusdan NA, Timmiati SN, Isahak WN, Yaakob Z, Lim KL, Khaidar D. Recent application of core-shell nanostructured catalysts for CO_2 thermocatalytic conversion processes. Nanomaterials. 2022; 12: 3877.
155. Rasul MG, Ahmed S, Sattar MA, Jahirul MI. Hydrodynamic performance assessment of photocatalytic reactor with baffles and roughness in the flow path: A modelling approach with experimental validation. Heliyon. 2023; 9: e19623.
156. Nalla BT, Choudhary BK, Sunil Kumar M, Ramachandra CG, Vaghela DR, Pradhan P, et al. Nanocatalyst-enabled waste-to-energy systems: From material innovation to techno-economic and sustainability pathways. Rev Inorg Chem. 2025. doi: 10.1515/revic-2025-0076.